Toll-like receptors (TLRs) and differentiate into mature DCs. The mature DCs strongly express major histocompatibility complex (MHC) class II and costimulatory molecules on the surface, which are associated with high antigen presentation ability. The mature DCs leave the peripheral tissue, migrate to the T-cell areas of draining lymphoid organs, and activate antigen-specific helper T cells and induce their differentiation into T helper type 1 (Th1), Th2 or Th17 cells.[4,5] These Th cells initiate appropriate acquired immunity for eradication of the pathogens.

DCs produce various cytokines upon stimulation with pathogen products such as lipopolysaccharide (LPS) and lipoproteins via TLRs.[3,6] The cytokines produced by DCs affect the balance between Th1, Th2 and Th17 differentiation in the process of antigen presentation. Interleukin (IL)-12 and IL-23, members of the IL-12 cytokine family,[7,8] are representative of the cytokines produced by DCs. These cytokines are heterodimeric proteins and share a common chain, IL-12 p40. The common p40 chain combines with the IL-12p35 or IL-23p19 chain to produce IL-12 or IL-23, respectively. Of note, the functions of these cytokines are entirely different. IL-12 promotes differentiation of Th1 cells, which are responsible for cell-mediated immunity, and inhibits Th17 cell activity via interferon (IFN)-γ production.[9,10] In contrast, IL-23 enhances the activity of Th17 cells, which promote inflammatory responses and appear to be responsible for the pathogenesis of certain autoimmune disorders.[11,12]

It has been reported that IL-12 and IL-23 production is differentially regulated in DCs stimulated with different TLR ligands. Thus, the balance between IL-12 and IL-23 produced by DCs is crucial for induction of appropriate immune responses (i.e. Th1 versus Th17 responses).

Prostaglandins, endogenous lipid mediators including prostaglandin D_2 (PGD_2), PGE_2, PGF_2 and PGI_2, are produced by the sequential actions of cyclooxygenases and prostaglandin synthetases in response to various inflammatory stimuli.[13,14] In particular, PGE_2 plays an important role in inflammatory responses. PGE_2 induces pyrexia, hyperalgesia, and arterial dilation, which increases blood flow to inflamed tissues and results in oedema and enhanced microvascular permeability. PGE_2 also influences the functions of various immune cells, such as T cells, B cells, macrophages and DCs.[15–17] It has been reported that PGE_2 inhibits DC production of IL-12 but not IL-23 upon TLR stimulation.[18–20] However, the molecular mechanism underlying the PGE_2-mediated regulation of the production of these cytokine by DCs has not been elucidated in detail.

The effect of PGE_2 on already differentiated DCs has been extensively studied. However, the role of this mediator in DC differentiation is not well documented. Using bone marrow-derived DCs (BMDCs), we examined the effect of PGE_2 treatment on DC differentiation and the subsequent functions of mature DCs, focusing on the relationship between their ability to produce cytokines and the activities of phosphatidylinositol 3-kinase (PI3K)/Akt, mitogen-activated protein kinase (MAPK), and nuclear factor κB (NF-κB) pathways in response to TLR stimulation. We report herein that DC differentiation with PGE_2 results in the selective attenuation of the extracellular signal-related kinase (ERK) pathway, which may lead to a reduced ability to produce IL-23 but not IL-12.

Materials and methods

Reagents and antibodies (Abs)

Murine recombinant granulocyte–macrophage colony-stimulating factor (GM-CSF) was purchased from PeproTech (Rocky Hill, NJ). Rabbit complement (Low Tox-M) was purchased from Cedarlane (ON, Canada). Synthetic PGE_2 (> 99%) was purchased from Sigma-Aldrich (St Louis, MO). We tested the effect of PGE_2 using two different batches and confirmed that the two bathes had similar effects. Highly purified LPS (ultra-pure LPS) from *Escherichia coli* O111:B4 and Pam3CSK4 (P3C), a synthetic lipopeptide, were purchased from InvivoGen (San Diego, CA). Fluorescein isothiocyanate (FITC)-conjugated anti-mouse CD86 monoclonal Ab (mAb) (GL1), phycoerythrin (PE)-conjugated anti-mouse CD40 mAb (3/23), biotin-conjugated anti-I-A^b mAb (AF6-120·1), and streptavidin-conjugated peridinin chlorophyll protein (PerCP) were obtained from BD Biosciences (San Diego, CA). Anti-phospho-ERK1/2 (Thr^{202}/Tyr^{204}) Ab, anti-phospho-p38 MAPK (Thr^{180}/Tyr^{182}) Ab, anti-phospho-c-jun N-terminal kinase 1/2 (JNK1/2) (Thr^{183}/Tyr^{185}) mAb (81E11), anti-phospho-Akt (Ser^{473}) Ab, anti-phospho-NF-κB (Ser^{536}) mAb (93H1), anti-ERK1/2 mAb (137F5), and anti- glyceraldehyde-3-phosphate dehydrogenase (GAPDH) mAb (14C10) were purchased from Cell Signaling Technology (Beverly, MA).

Culture media

RPMI-1640 liquid medium was purchased from Sigma-Aldrich and supplemented with 100 IU/ml penicillin, 100 μg/ml streptomycin, 50 μM 2-mercaptoethanol and 5% fetal calf serum (FCS).

DC culture

Murine BMDCs were generated by a well-established method as previously described.[21–23] Bone marrow cells were prepared from femur and tibial bone marrow of C57BL/6 mice purchased from Japan SLC Inc. (Hamamatsu, Japan). After lysis of erythrocytes, MHC class II-, CD45R (B220)-, CD4- and CD8-positive cells were removed by killing with mAbs (1E4, RA3-6B2, GK1·5 and 53-6·7) and rabbit complement. The cells were thoroughly

washed to remove the mAbs, complement and cell debris. The cells were cultured in RPMI-1640 containing 5% FCS and GM-CSF (20 ng/ml) with or without PGE_2 (1 μM), at a density of 1×10^6 cells/ml/well (24-well plate). On day 2, the medium was carefully exchanged for fresh medium. On day 4, non-adherent granulocytes were removed without dislodging clusters of developing DCs, and fresh medium was added. On day 6, free-floating and loosely adherent cells were collected and were used as BMDCs. BMDCs cultured with GM-CSF alone or GM-CSF plus PGE_2 are referred to as cont-DC or PG-DC, respectively.

Cytokine measurement in culture supernatants

DCs were treated with the indicated combinations of TLR ligands for 24 hr in 5% FCS RPMI-1640 at a density of 1×10^6 cells/200 μl/well (96-well plate). P3C and LPS were used at 100 ng/ml and 1 μg/ml, respectively. The dose of each TLR ligand was determined on the basis of our preliminary dose–response study (data not shown) and a previous study.[23] In some experiments, cells were pretreated with U0126 (10 μM), a MAPK/ERK kinase (MEK)1/2-specific inhibitor, or vehicle [0·02% dimethyl sulphoxide (DMSO)] for 1 hr and then treated with LPS (1 μg/ml) and P3C (100 ng/ml) for 24 hr in the presence of the inhibitor or vehicle, respectively. The culture supernatants were subjected to quantification of the protein level of IL-12 (p70) and IL-23 by enzyme-linked immunosorbent assay (ELISA). The ELISA kits for IL-12 (p70) and IL-23 were purchased from BD Biosciences and eBioscience (San Diego, CA), respectively.

Flow cytometry

The cells were incubated with 2·4G2 (rat anti-mouse Fcγ receptor III/II, CD16/CD32) supernatant to prevent binding of specific mAb to Fcγ receptor III/II and then stained with FITC-, PE-, or biotin-conjugated mAb and streptavidin-PerCP. Flow cytometric analysis was performed on EPICS XL (Beckman Coulter Inc., Miami, FL) as previously described.[23]

Immunoblotting

Cont-DCs and PG-DCs were treated with LPS (1 μg/ml) and P3C (100 ng/ml) for 15 or 30 min at a density of 1×10^6 cells/ml/well (24-well plate). In some experiments, cells were pretreated with U0126 (10 μM) or vehicle (0·02% DMSO) alone for 1 hr and then treated with LPS (1 μg/ml) and P3C (100 ng/ml) in the presence of the inhibitor or vehicle, respectively. Rapid cooling of the cells on ice halted the reactions, and these cells were washed with ice-cold phosphate-buffered saline. The whole cell lysates were prepared using cell lysis buffer (Cell Signaling Technology). The cell lysates were separated by sodium dodecyl sulphate–polyacrylamide gel electrophoresis (SDS-PAGE), and then blotted onto a polyvinylidene fluoride membrane (Millipore, Bedford, MA). The membrane was probed with the primary Ab and developed with the horseradish peroxidase-conjugated secondary Ab by enhanced chemiluminescence.[23]

Results

Expression of surface molecules on DCs generated with or without PGE_2

BMDCs were generated by a well-established method as previously described.[21–23] Bone marrow cells were prepared from murine femur and tibial bone marrow and MHC class II-, CD45R (B220)-, CD4- and CD8-positive cells were removed to prevent an indirect influence of PGE_2 via these lineage marker-positive cells in the DC generation. The lineage marker-negative cells were cultured with GM-CSF alone or GM-CSF plus PGE_2 for 6 days and used as cont-DCs or PG-DCs, respectively. There was no difference in viability between cont-DCs and PG-DCs (data not shown). Both cont-DCs and PG-DCs showed an immature DC phenotype and were CD11c positive, with low expression of CD40 and CD86 and moderate expression of $I\text{-}A^b$ (Fig. 1a). Although the levels of $I\text{-}A^b$ and CD40 expression of PG-DCs were slightly lower than those of cont-DCs, no significant differences were detected in the expression levels of these molecules between the two types of cell (Fig. 1b,c).

Effect of PGE_2 treatment on IL-12 and IL-23 production by DCs upon TLR stimulation

We first examined the effect of PGE_2 on IL-12 and IL-23 production by the differentiated DCs upon TLR stimulation. Cont-DCs were treated with ultra-pure LPS (a TLR4 ligand) and/or P3C, a synthetic lipopeptide (a TLR2/1 ligand), for 24 hr in the presence or absence of PGE_2, and the production of IL-12 (p70) and IL-23 was measured by ELISA (Fig. 2a). Compared with the control culture, IL-12 production by cont-DCs was moderately or slightly increased by treatment with LPS or P3C, respectively (Fig. 2a left). Simultaneous treatment of the cont-DCs with LPS and P3C resulted in synergistically increased production of IL-12. In contrast, IL-23 production by cont-DCs was markedly increased by treatment with LPS (Fig. 2a right). Although P3C showed only a slight effect on IL-23 production by cont-DCs, this ligand enhanced LPS-induced IL-23 production. The addition of PGE_2 to the culture during TLR stimulation completely inhibited IL-12 production by cont-DCs upon LPS and/or P3C stimulation (Fig. 2a left), but showed no significant effects on IL-23 production (Fig. 2a right).

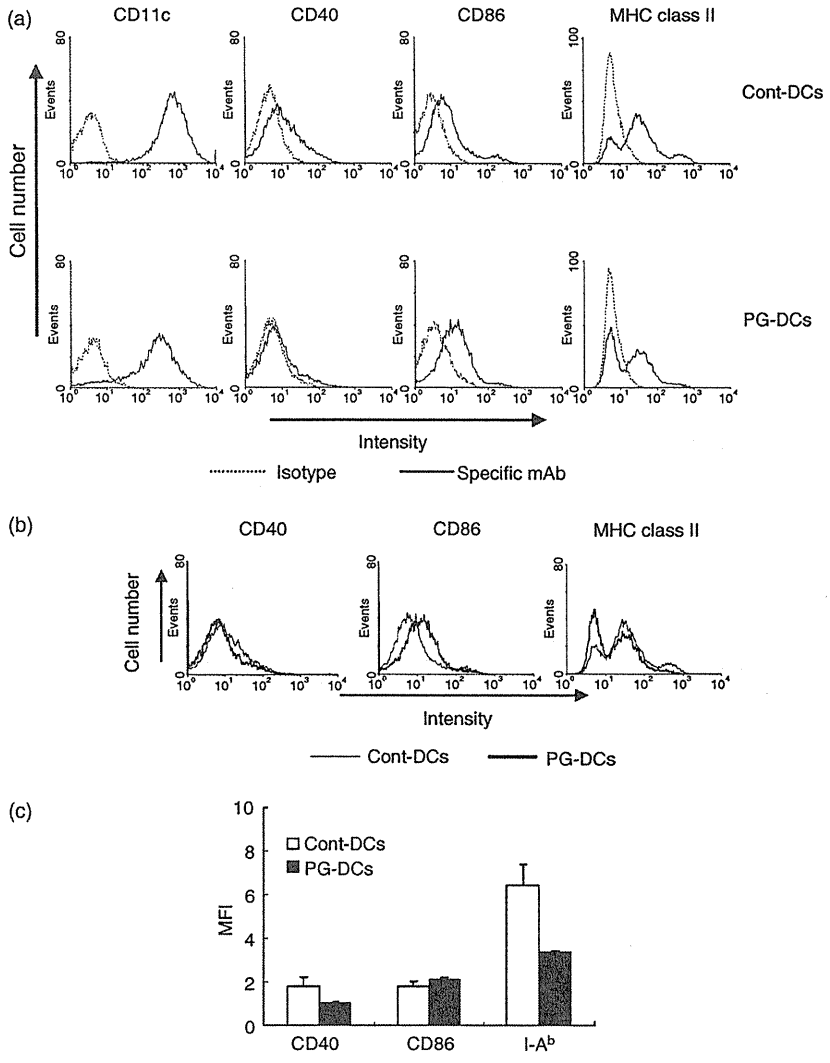

Figure 1. Expression of surface molecules on dendritic cells (DCs) generated with or without prostaglandin E_2 (PGE_2). Bone marrow-derived DCs were generated by culturing murine bone marrow cells with granulocyte–macrophage colony-stimulating factor (GM-CSF) alone or GM-CSF plus PGE_2, and these cells are referred to as 'cont-DCs' or 'PG-DCs', respectively. The cell surface expression of CD11c, CD40, CD86 and I-A^b was analysed by flow cytometry. (a, b) Representative histograms from three independent experiments. (c) The mean fluorescence intensity (MFI) of the cells. Each column represents the mean ± standard error of three independent experiments. mAb, monoclonal antibody; MHC, major histocompatibility complex.

To investigate the effect of PGE_2 on DC differentiation and functions, we next compared IL-12 and IL-23 production in response to TLR ligands between cont-DCs and PG-DCs. Both types of DC were treated with LPS and/or P3C for 24 hr and levels of IL-12 and IL-23 were determined (Fig. 2b). Cont-DCs again showed substantial IL-12 production upon LPS plus P3C stimulation (Fig. 2b left). In response to LPS and/or P3C treatment, PG-DCs also produced substantial IL-12, similar to that produced by cont-DCs. Upon P3C stimulation, IL-12 production by PG-DCs was slightly higher than that by cont-DCs. However, upon stimulation with LPS alone or LPS plus P3C, no significant difference was detected in IL-12 production between cont-DCs and PG-DCs. In contrast, IL-23 production by PG-DCs in response to LPS or LPS plus P3C was significantly suppressed compared with that by cont-DCs (Fig. 2b right). Thus, the influence of PGE_2 on the production of IL-12 and IL-23 by DCs appeared to be dependent on the differentiation state of the DCs.

It has been reported that PGE_2 also influences IL-10 production.[20] We thus compared cont-DCs and PG-DCs in terms of their ability to produce IL-10 in response to TLR stimulation. We found that IL-10 production by PG-DCs was markedly higher than that by cont-DCs (Fig. 2c).

We also analysed CD40, CD86 and I-A^b expression on cont-DCs and PG-DCs following LPS plus P3C

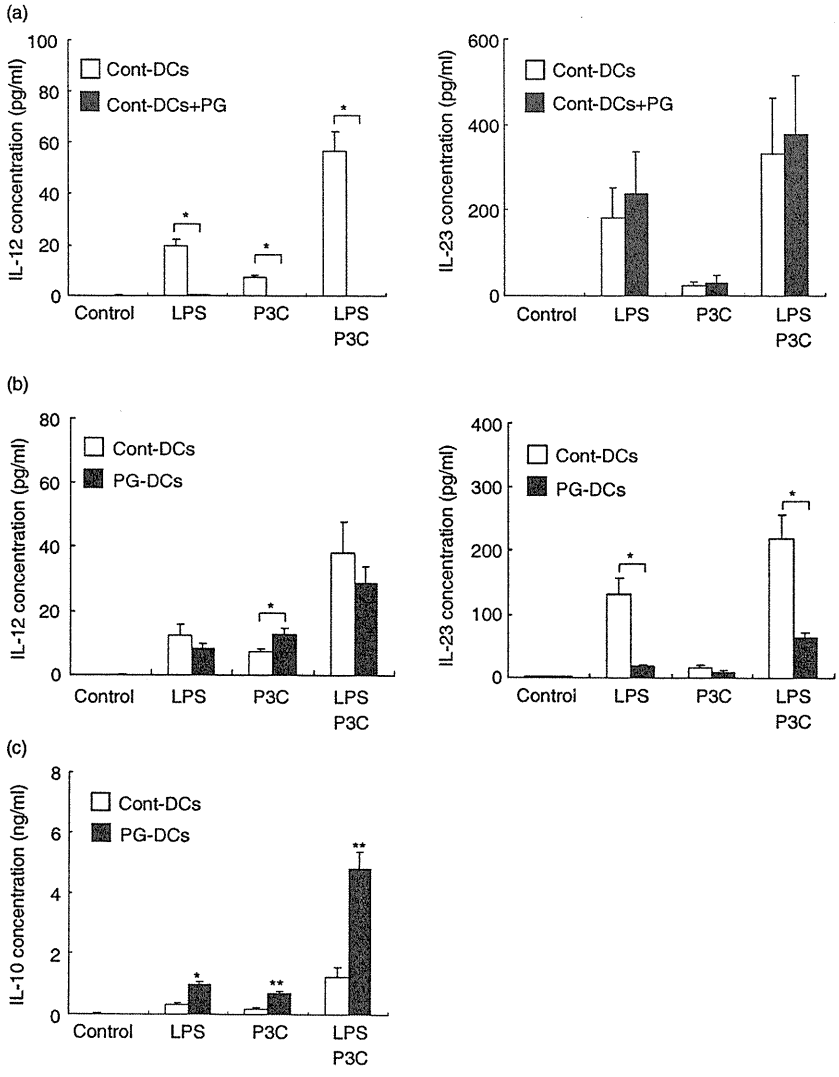

Figure 2. Effects of prostaglandin E_2 (PGE_2) on interleukin (IL)-12 and IL-23 production by dendritic cells (DCs) upon Toll-like receptor (TLR) stimulation. Bone marrow-derived DCs were generated by culturing murine bone marrow cells with granulocyte–macrophage colony-stimulating factor (GM-CSF) alone or GM-CSF plus PGE_2, and these cells are referred to as 'cont-DCs' or 'PG-DCs', respectively. (a) The cont-DCs were treated with lipopolysaccharide (LPS) and/or Pam3CSK4 (P3C) in the presence (Cont-DCs+PG) or absence (Cont-DCs) of PGE_2 for 24 hr. (b, c) The cont-DCs and PG-DCs were treated with LPS and/or P3C for 24 hr. The amounts of IL-12, IL-23 (b), and IL-10 (c) in the culture supernatants were quantified by enzyme-linked immunosorbent assay (ELISA). Statistical significance was calculated using Student's *t*-test (*$P < 0{\cdot}05$).

stimulation. Cont-DCs and PG-DCs showed similar expression profiles even after TLR stimulation (data not shown).

TLR2 and TLR4 expression on cont-DCs and PG-DCs

The ability of PG-DCs to produce IL-23 but not IL-12 was significantly lower than that of cont-DCs upon LPS and P3C stimulation (Fig. 2b). We speculated that treatment with PGE_2 during DC generation might affect the pattern of TLR2 and TLR4 expression on the DCs, resulting in a different pattern of cytokine production. We thus analysed and compared the cell surface expression of TLR2 and TLR4 on cont-DCs and PG-DCs by flow cytometry (Fig. 3). TLR2 and TLR4 were detected on both types of DC (Fig. 3a). There was no significant difference in the level of these TLRs between cont-DCs and PG-DCs (Fig. 3b).

Akt, MAPK, and NF-κB activation in cont-DCs and PG-DCs upon TLR stimulation

TLR ligands activate the PI3K/Akt, MAPK and NF-κB pathways in macrophages and DCs.[24,25] These pathways play crucial roles in the regulation of cytokine production. Figures 2 and 3 demonstrate that PGE_2 treatment during DC generation decreased production of IL-23 by DCs but not that of IL-12 in response to LPS plus P3C,

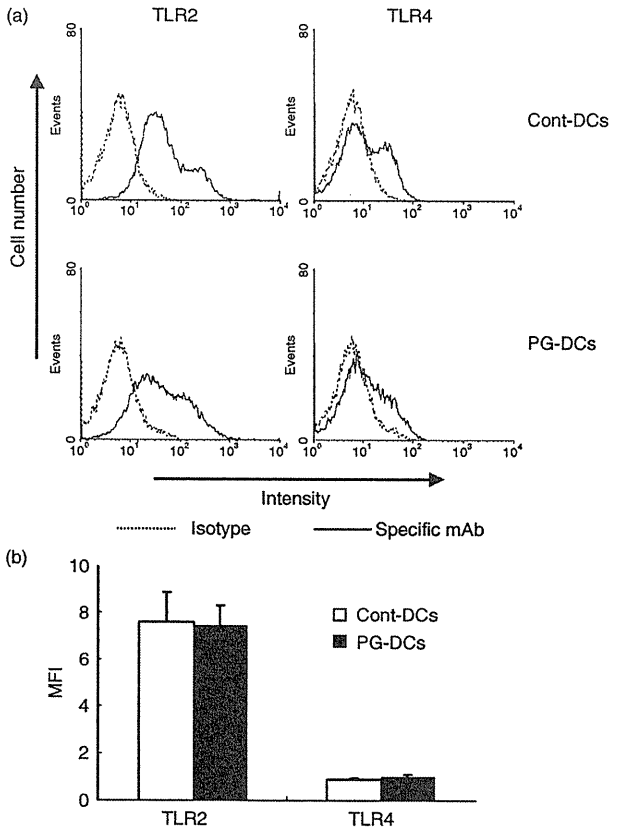

Figure 3. Effects of prostaglandin E_2 (PGE_2) treatment during dendritic cell (DC) differentiation on Toll-like receptor 2 (TLR2) and TLR4 expression on the differentiated DCs. Bone marrow-derived DCs were generated by culturing murine bone marrow cells with granulocyte–macrophage colony-stimulating factor (GM-CSF) alone or GM-CSF plus PGE_2, and these cells are referred to as 'cont-DCs' or 'PG-DCs', respectively. The cell surface expression of TLR2 and TLR4 on cont-DCs and PG-DCs was analysed by flow cytometry. (a) A representative histogram from three independent experiments. (b) The mean fluorescence intensity (MFI) of the cells. Each column represents the mean ± standard error of three independent experiments. mAb, monoclonal antibody.

without affecting the cell surface expression of TLR2 and TLR4. These findings suggest that the PGE_2 treatment modifies the intracellular signal pathway following TLR stimulation. We then analysed and compared the activities of the PI3K/Akt, MAPK and NF-κB pathways in cont-DCs and PG-DCs.

We previously demonstrated that Akt, MAPKs (ERK1/2, p38 MAPK and JNK1/2), and NF-κB p65 were significantly activated in BMDCs following LPS plus P3C stimulation, and the activity of these molecules reached a peak at 15–30 min after the stimulation.[26,27] The activation levels declined after 60 min. Hence, cont-DCs and PG-DCs were treated with LPS plus P3C for 15 and 30 min and the intracellular protein levels of the active forms of these molecules, phospho-Akt (pAkt), phospho-ERK1/2 (pERK), phospho-p38 MAPK (pp38), phospho-JNK1/2 (pJNK) and phospho-NF-κB p65 (pp65), were determined by immunoblotting (Fig. 4). Marked phosphorylation of ERK1/2, p38 MAPK and JNK1/2 was observed in both types of DC at 15 and 30 min after the TLR stimulation (Fig. 4a). No significant differences were detected in the levels of pAkt, pp38, pJNK1/2 and pp65 between cont-DCs and PG-DCs (Fig. 4b). Notably, however, the level of pERK1/2 in PG-DCs at 30 min after the stimulation was significantly lower than that in cont-DCs, although no difference was found in total ERK1/2 level between these two types of cell (Fig. 4b right). Thus, PGE_2 treatment during DC generation selectively affected activation of ERK1/2 in the resultant mature DCs in response to the TLR ligands.

The effect of ERK1/2 inhibition on IL-12 and IL-23 production by DCs upon TLR stimulation

The prior results (Fig. 4) suggested that the decreased ERK1/2 activity in PG-DCs might be related to their impaired IL-23 production upon TLR stimulation. We next focused on the role of the ERK1/2 pathway in IL-23 production using U0126, a specific inhibitor of the MEK1/2–ERK1/2 pathway. BMDCs (cont-DCs) were pretreated with U0126 (10 μM) or vehicle (0·02% DMSO) alone for 1 hr and then treated with LPS plus P3C for 24 hr in the presence of U0126 or vehicle, respectively. IL-12 and IL-23 production was again markedly increased by stimulation with LPS plus P3C (Fig. 5a). The vehicle treatment showed no effect on the production of these cytokines. Compared with the control culture, treatment with U0126 markedly increased IL-12 production, but significantly reduced IL-23 production by DCs stimulated with LPS plus P3C. These findings demonstrate that the ERK pathway is involved in the regulation of IL-12 and IL-23 produced by DCs in response to TLR stimulation.

We then confirmed the effect of U0126 on the activities of ERK1/2 and other signal molecules in DCs stimulated with LPS plus P3C. BMDCs were pretreated with U0126 or vehicle alone for 1 hr and then treated with LPS plus P3C for 15 min in the presence of U0126 or vehicle, respectively. The intracellular protein levels of pAkt, pERK1/2, pp38, pJNK and pp65 were determined by immunoblotting. U0126 completely inhibited ERK1/2 phosphorylation (Fig. 5b) in DCs upon TLR stimulation without affecting the levels of pAkt, pp38, pJNK and pp65 (data not shown). Thus, U0126 selectively inhibited ERK1/2 activation, and the ERK1/2 pathway appeared to be dispensable for the activation of other signal molecules in DCs stimulated with LPS plus P3C.

Discussion

Autoreactive Th cells induce tissue damage and inflammation, which is involved in the pathogenesis of various

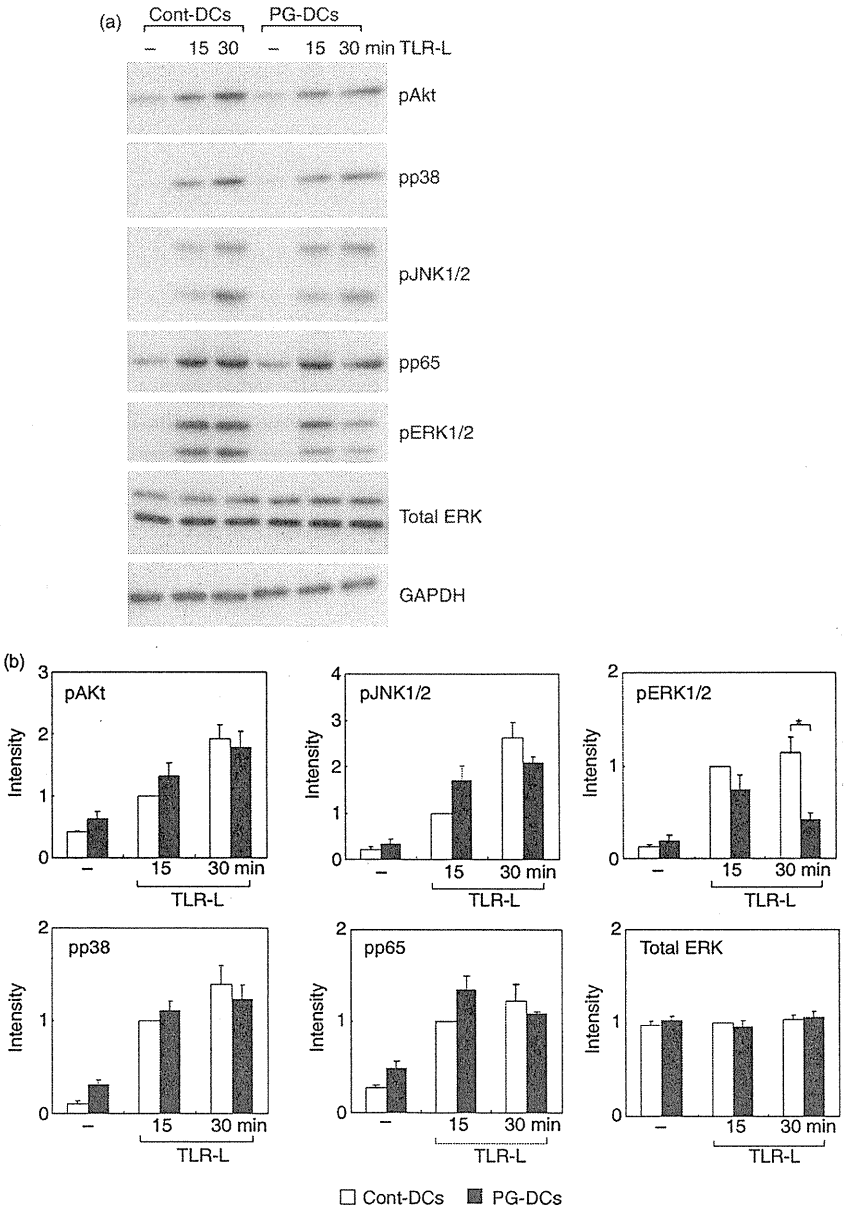

Figure 4. Effects of prostaglandin E_2 (PGE_2) treatment during dendritic cell (DC) differentiation on the activation of the Akt, mitogen-activated protein kinase (MAPK), and nuclear factor κB (NF-κB) pathways in the differentiated DCs in response to Toll-like receptor (TLR) stimulation. Bone marrow-derived DCs were generated by culturing murine bone marrow cells with granulocyte–macrophage colony-stimulating factor (GM-CSF) alone or GM-CSF plus PGE_2, and these cells are referred to as 'cont-DCs' or 'PG-DCs', respectively. The cont-DCs and PG-DCs were treated with lipopolysaccharide (LPS) plus Pam3CSK4 (P3C) [TLR ligands (TLR-L)] for 15 or 30 min. The intracellular protein levels of phospho-Akt (pAkt), phospho-extracellular signal-related kinase 1/2 (pERK1/2), phospho-p38 MAPK (pp38), phospho-c-jun N-terminal kinase 1/2 (pJNK1/2), phospho-nuclear factor (NF)-κB p65 (pp65), total ERK, and glyceraldehyde-3-phosphate dehydrogenase (GAPDH) were determined by immunoblotting. (a) A representative immunoblot from three independent experiments is shown. (b) The relative intensity of the specific band is shown. Each column represents the mean ± standard error of three independent experiments. Statistical significance was calculated using Student's *t*-test ($^*P < 0{\cdot}05$).

immune diseases. Recent studies suggest that Th17 cells are responsible for inflammation and autoimmunity,[28,29] whereas Th1 cells have protective effects on autoimmune responses in certain conditions.[30–32] Th1 and Th17 cells are characterized by their expression of IFN-γ and IL-17, respectively.[28,29] Th1 differentiation is induced by IL-12, while Th17 differentiation is enhanced by IL-23 following the initiation of this differentiation by transforming growth factor-β and IL-6. Thus, the roles of IL-12 and IL-23 in Th differentiation are entirely different, although these cytokines, members of IL-12 family, have similar structures.[7,8]

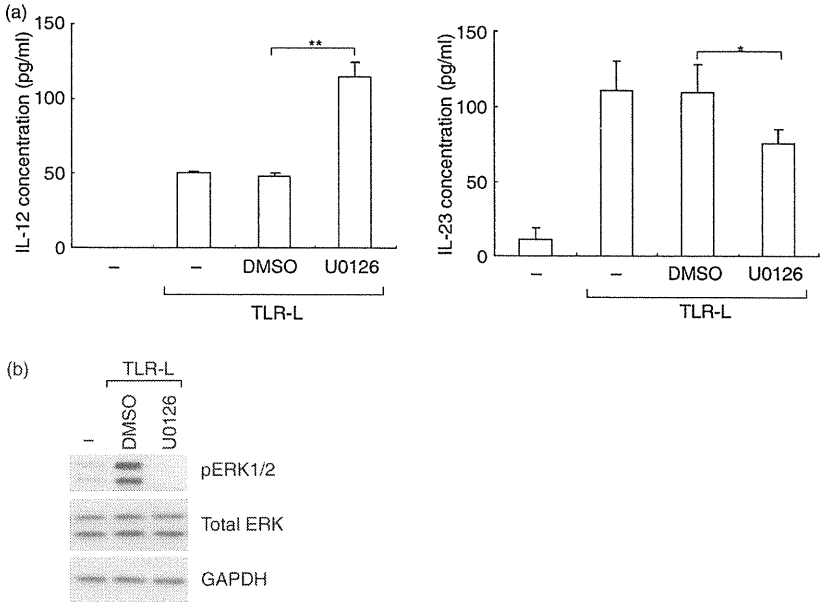

Figure 5. The effect of extracellular signal-related kinase 1/2 (ERK1/2) inhibition on interleukin (IL)-12 and IL-23 production by dendritic cells (DCs) upon Toll-like receptor (TLR) stimulation. Bone marrow-derived DCs were generated by culturing murine bone marrow cells with granulocyte–macrophage colony-stimulating factor (GM-CSF). (a) The DCs were pretreated with U0126 (10 μM), a specific inhibitor of the MAPK/ERK kinase (MEK)1/2–ERK1/2 pathway, or vehicle [0·05% dimethyl sulphoxide (DMSO)] for 1 hr and then treated with lipopolysaccharide (LPS) plus Pam3CSK4 (P3C) [TLR ligands (TLR-L)] for 24 hr in the presence of U0126 or vehicle, respectively. The amounts of IL-12 and IL-23 in the culture supernatants were quantified by enzyme-linked immunosorbent assay (ELISA). Statistical significance was calculated using Student's *t*-test (*$P < 0.05$; ** $P < 0.005$). (b) The DCs were pretreated with U0126 (10 μM) or vehicle alone (0·05% DMSO) for 1 hr and then treated with LPS plus P3C for 15 min in the presence of ERK1/2 inhibitor or vehicle (DMSO), respectively. The intracellular protein levels of phospho-ERK1/2, total ERK, and glyceraldehyde-3-phosphate dehydrogenase (GAPDH) were determined by immunoblotting. A representative immunoblot from three independent experiments is shown.

Although PGE_2 promotes inflammatory responses, this mediator regulates the functions of immune cells, including T cells, B cells, macrophages and DCs.[15–17] It has been reported that PGE_2 induces apoptosis of developing and resting T cells,[33,34] but protects T cells from the apoptosis induced by TCR-mediated activation.[35] In contrast, PGE_2 had a positive effect, or no effect, on the proliferation of mature B cells, but suppressed the proliferation of immature B cells.[36] It seems that the effects of PGE_2 are dependent on the developmental or maturation state of the cells.

In the present study, we examined IL-12 and IL-23 production in DCs treated with PGE_2 during differentiation from bone marrow cells as well as in differentiated DCs treated with PGE_2 during activation with TLR ligands. PGE_2 treatment during DC activation by TLR ligands completely inhibited the TLR-mediated production of IL-12 by DCs, but not that of IL-23. This cytokine shift in DCs appears to drive Th17 differentiation.[18,19] In contrast, PGE_2 treatment during differentiation of DCs from bone marrow cells resulted in reduced DC production of IL-23, but not IL-12, in response to the TLR ligands. We thus concluded that PGE_2 was a key molecule in controlling the balance of IL-12 and IL-23 production by DCs and that the effect was dependent on the developmental or maturational state of the DCs, as reported in studies of T and B cells.[33–36]

We next focused on the mechanism underlying the decreased ability to produce IL-23 in response to TLR2 and TLR4 ligands of DCs pretreated with PGE_2 during their differentiation (PG-DCs). As PGE_2 treatment during DC differentiation never affected the cell surface expression of TLR2 and TLR4, we postulated that PGE_2 influenced the intracellular signal transduction system of the DCs. Intracellular signal pathways via PI3K/Akt, MAPK (ERK1/2, p38 MAPK and JNK1/2) and NF-κB play crucial roles in the regulation of cytokine production. It has been reported that the PI3K and ERK1/2 pathways negatively regulate IL-12 production,[37–40] while the p38 MAPK and NF-κB pathways are responsible for the production of inflammatory cytokines, including IL-12.[25,41,42] We found that PGE_2 treatment during DC differentiation resulted in marked attenuation of ERK1/2 activity in the DCs upon TLR2 and TLR4 stimulation. However, no significant effects were detected on the activity of other signal molecules (Akt, p38 MAPK, JNK1/2 and NF-κB p65). In addition, blocking the ERK1/2 pathway with U0126 significantly inhibited IL-23 production by DCs.

Thus, the attenuation of ERK1/2 activity in the PG-DCs appeared to be at least partly responsible for their reduced IL-23 production. However, the inhibitory effect of the ERK1/2 inhibitor U0126 on IL-23 production by cont-DCs was weaker than that on IL-23 production by PG-DCs. It seems that complex mechanisms other than attenuation of the activity of the ERK1/2 pathway are involved in the impaired ability of PG-DCs to produce IL-23.

In contrast, ERK1/2 inhibition with U0126 significantly enhanced IL-12 production by cont-DCs upon TLR stimulation. However, IL-12 production by PG-DCs upon TLR stimulation was never enhanced compared with that by cont-DCs. ERK1/2 activity in PG-DCs was significantly lower than that in cont-DCs at 30 min but not 15 min after TLR stimulation. Thus, ERK1/2 inhibition at the early time-point (at 15 min) might be required for increased IL-12 production. Alternatively, other unknown mechanisms might be involved in the effect of reduced ERK activity on IL-12 production in PG-DCs.

In contrast to the present study, Khayrullina *et al.* [20] recently showed that PGE_2 treatment during BMDC differentiation resulted in enhanced IL-23 production by the DCs upon LPS stimulation. In the present study, MHC class II-, CD45R (B220)-, CD4- and CD8-positive cells were removed from the bone marrow cell culture to prevent indirect effects of PGE_2 on DC functions via these lineage marker-positive cells. However, these lineage marker-positive cells were not absent from the culture used for DC differentiation with PGE_2 in the study by Khayrullina *et al.*[20] As already described, PGE_2 influences a variety of immune cells. It seems possible that indirect effects of PGE_2 via these lineage marker-positive cells, such as T cells, B cells and macrophages, influenced DC differentiation. The lymphocytes may have provided costimulation signals which drove IL-23 production, or perhaps there were non-myeloid sources of IL-23 in the DC culture. Furthermore, we used highly purified (ultrapure) LPS for DC activation, while Khayrullina *et al.* [20] used standard LPS, which contains TLR ligands other than LPS.[26,43] Thus, the discrepancy between the results of the present study and those of Khayrullina *et al.* [20] may be attributable to differences in the culture system and/or the DC stimulant used.

We also examined IL-10 production by DCs upon TLR stimulation and found that production was markedly increased by treatment with PGE_2 during DC development. Thus, it seems that PGE_2 negatively regulates inflammatory responses by not only suppressing IL-23 production but also enhancing IL-10 production.

It has been suggested that PGE_2 not only promotes inflammatory responses but also exhibits anti-inflammatory properties, including negative regulation of immune cell functions.[16] In the present study we have demonstrated that PGE_2 has an anti-inflammatory effect mediated by the attenuation of the production of IL-23 by DCs, which promotes Th17-mediated inflammatory responses. We also showed that DCs treated with PGE_2 during differentiation produce a large amount of IL-10. Physiologically, these effects of PGE_2 may contribute to negative feedback regulation that suppresses undesirable chronic inflammation. As the balance between IL-12 and IL-23 produced by DCs is crucial for the regulation of inflammatory and immune responses, further elucidation of the mechanism underlying the PGE_2-mediated regulation of the IL-12 and IL-23 balance may lead to the development of clinical applications exploiting this new regulation system for the treatment of various infectious diseases and immune disorders.

Acknowledgements

This study was supported in part by a Grant-in-Aid for Scientific Research (B) from the Japan Society for the Promotion of Science (JSPS), the Global COE Program 'Establishment of International Collaboration Center for Zoonosis Control' from the Ministry of Education, Culture, Science, Sports and Technology (MEXT) and a Grant for Researchers on Behçet's Disease, Ministry of Health, Labour and Welfare, Japan.

Disclosures

The authors have no financial conflict of interest.

References

1 Steinman R. The dendritic cell system and its role in immunogenicity. *Annu Rev Immunol* 1991; 9:271–96.
2 Hart DNJ. Dendritic cells: unique leukocyte populations which control the primary immune response. *Blood* 1997; 90:3245–87.
3 Banchereau J, Steinman RM. Dendritic cells and the control of immunity. *Nature* 1998; 392:245–51.
4 Cyster JG. Chemokines and cell migration in secondary lymphoid organs. *Science* 1999; 286:2098–102.
5 Sallusto F, Lanzavecchia A. Understanding dendritic cell and T-lymphocyte traffic through the analysis of chemokine receptor expression. *Immunol Rev* 2000; 177:134–40.
6 Pearce EJ, Kane CM, Sun JR. Regulation of dendritic cell function by pathogen-derived molecules plays a key role in dictating the outcome of the adaptive immune response. *Chem Immunol Allergy* 2006; 90:82–90.
7 Goriely S, Neurath MF, Goldman M. How microorganisms tip the balance between interleukin-12 family members. *Nat Rev Immunol* 2008; 8:81–6.
8 Goriely S, Goldman M. The interleukin-12 family: new players in transplantation immunity? *Am J Transplant* 2007; 7:278–84.
9 Harrington LE, Hatton RD, Mangan PR, Turner H, Murphy TL, Murphy KM, Weaver CT. Interleukin 17-producing $CD4^+$ effector T cells develop via a lineage distinct from the T helper type 1 and 2 lineages. *Nat Immunol* 2005; 6:1123–32.
10 Park H, Li Z, Yang XO *et al.* A distinct lineage of CD4 T cells regulates tissue inflammation by producing interleukin 17. *Nat Immunol* 2005; 6:1133–41.
11 Mangan PR, Harrington LE, O'Quinn DB *et al.* Transforming growth factor-β induces development of the T(H)17 lineage. *Nature* 2006; 441:231–4.
12 Bettelli E, Carrier Y, Gao W *et al.* Reciprocal developmental pathways for the generation of pathogenic effector TH17 and regulatory T cells. *Nature* 2006; 441:235–8.
13 Goetzl EJ, An S, Smith WL. Specificity of expression and effects of eicosanoid mediators in normal physiology and human diseases. *FASEB J* 1995; 9:1051–8.
14 Sugimoto Y, Narumiya S. Prostaglandin E receptors. *J Biol Chem* 2007; 282:11613–7.

15 Phipps RP, Stein SH, Roper RL. A new view of prostaglandin-E regulation of the immune response. *Immunol Today* 1991; 12:349–52.
16 Harris SG, Padilla J, Koumas L, Ray D, Phipps RP. Prostaglandins as modulators of immunity. *Trends Immunol* 2002; 23:144–50.
17 Sá-Nunes A, Bafica A, Lucas DA *et al.* Prostaglandin E_2 is a major inhibitor of dendritic cell maturation and function in *Ixodes scapularis* saliva. *J Immunol* 2007; 179:1497–505.
18 Sheibanie AF, Tadmori I, Jing H, Vassiliou E, Ganea D. Prostaglandin E_2 induces IL-23 production in bone marrow-derived dendritic cells. *FASEB J* 2004; 18:1318–20.
19 Sheibanie AF, Yen JH, Khayrullina T, Emig F, Zhang M, Tuma R, Ganea D. The proinflammatory effect of prostaglandin E_2 in experimental inflammatory bowel disease is mediated through the IL-23→IL-17 axis. *J Immunol* 2007; 178:8138–47.
20 Khayrullina T, Yen JH, Jing H, Ganea D. In vitro differentiation of dendritic cells in the presence of prostaglandin E_2 alters the IL-12/IL-23 balance and promotes differentiation of Th17 cells. *J Immunol* 2008; 181:721–35.
21 Inaba K, Inaba M, Romani N, Aya H, Deguchi M, Ikehara S, Muramatsu S, Steinman RM. Generation of large numbers of dendritic cells from mouse bone marrow cultures supplemented with granulocyte/macrophage colony-stimulating factor. *J Exp Med* 1992; 176:1693–702.
22 Yamazaki S, Bonito AJ, Spisek R, Dhodapkar M, Inaba K, Steinman RM. Dendritic cells are specialized accessory cells along with TGF-β for the differentiation of $Foxp3^+$ $CD4^+$ regulatory T cells from peripheral Foxp3 precursors. *Blood* 2007; 110:4293–302.
23 Yanagawa Y, Onoé K. Enhanced IL-10 production by TLR4- and TLR2-primed dendritic cells upon TLR restimulation. *J Immunol* 2007; 178:6173–80.
24 Kawai T, Akira S. Pathogen recognition with Toll-like receptors. *Curr Opin Immunol* 2005; 17:338–44.
25 Kawai T, Akira S. Signaling to NF-κB by Toll-like receptors. *Trends Mol Med* 2007; 13:460–9.
26 Hirata N, Yanagawa Y, Ebihara T *et al.* Selective synergy in anti-inflammatory cytokine production upon cooperated signaling via TLR4 and TLR2 in murine conventional dendritic cells. *Mol Immunol* 2008; 45:2734–42.
27 Hirata N, Yanagawa Y, Iwabuchi K, Onoé K. Selective regulation of interleukin-10 production via Janus kinase pathway in murine conventional dendritic cells. *Cell Immunol* 2009; 258:9–17.
28 Steinman L. A brief history of T_H17, the first major revision in the T_H1/T_H2 hypothesis of T cell-mediated tissue damage. *Nat Med* 2007; 13:139–45.
29 Korn T, Bettelli E, Oukka M, Kuchroo VK. IL-17 and T_H17 cells. *Annu Rev Immunol* 2009; 27:485–517.
30 Ferber IA, Brocke S, Taylor-Edwards C *et al.* Mice with a disrupted IFN-γ gene are susceptible to the induction of experimental autoimmune encephalomyelitis (EAE). *J Immunol* 1996; 156:5–7.
31 Vermeire K, Heremans H, Vandeputte M, Huang S, Billiau A, Matthys P. Accelerated collagen-induced arthritis in IFN-γ receptor-deficient mice. *J Immunol* 1997; 158:5507–13.
32 Manoury-Schwartz B, Chiocchia G, Bessis N *et al.* High susceptibility to collagen-induced arthritis in mice lacking IFN-γ receptors. *J Immunol* 1997; 158:5501–6.
33 Mastino A, Piacentini M, Grelli S, Favalli C, Autuori F, Tentori L, Oliverio S, Garaci E. Induction of apoptosis in thymocytes by prostaglandin E_2 in vivo. *Dev Immunol* 1992; 2:263–71.
34 Pica F, Franzese O, D'Onofrio C, Bonmassar E, Favalli C, Garaci E. Prostaglandin E_2 induces apoptosis in resting immature and mature human lymphocytes: a c-Myc-dependent and Bcl-2-independent associated pathway. *J Pharmacol Exp Ther* 1996; 277:1793–800.
35 Porter BO, Malek TR. Prostaglandin E_2 inhibits T-cell-activation-induced apoptosis and Fas-mediated cellular cytotoxicity by blockade of Fas-ligand induction. *Eur J Immunol* 1999; 29:2360–5.
36 Garrone P, Galibert L, Rousset F, Fu SM, Banchereau J. Regulatory effects of prostaglandin E_2 on the growth and differentiation of human B lymphocytes activated through their CD40 antigen. *J Immunol* 1994; 152:4282–90.
37 Fukao T, Tanabe M, Terauchi Y *et al.* PI3K-mediated negative feedback regulation of IL-12 production in DCs. *Nat Immunol* 2002; 3:875–81.
38 Puig-Kröger A, Relloso M, Fernández-Capetillo O, Zubiaga A, Silva A, Bernabéu C, Corbí AL. Extracellular signal-regulated protein kinase signaling pathway negatively regulates the phenotypic and functional maturation of monocyte-derived human dendritic cells. *Blood* 2001; 98:2175–82.
39 Yanagawa Y, Iijima N, Iwabuchi K, Onoé K. Activation of extracellular signal-related kinase by TNF-α controls the maturation and function of murine dendritic cells. *J Leukoc Biol* 2002; 71:125–32.
40 Agrawal S, Agrawal A, Doughty B, Gerwitz A, Blenis J, Van Dyke T, Pulendran B. Cutting edge: different Toll-like receptor agonists instruct dendritic cells to induce distinct Th responses via differential modulation of extracellular signal-regulated kinase-mitogen-activated protein kinase and c-Fos. *J Immunol* 2003; 171:4984–9.
41 Saccani S, Pantano S, Natoli G. p38-Dependent marking of inflammatory genes for increased NF-κB recruitment. *Nat Immunol* 2002; 3:69–75.
42 Re F, Strominger JL. Toll-like receptor 2 (TLR2) and TLR4 differentially activate human dendritic cells. *J Biol Chem* 2001; 276:37692–9.
43 Hirschfeld M, Ma M, Weis JH, Vogel SN, Weis JJ. Cutting edge: repurification of lipopolysaccharide eliminates signaling through both human and murine toll-like receptor 2. *J Immunol* 2000; 165:618–22.

Identification of a third variable lymphocyte receptor in the lamprey

Jun Kasamatsu[a,1,2], Yoichi Sutoh[a,1], Kazunori Fugo[a], Noriyuki Otsuka[a], Kazuya Iwabuchi[b], and Masanori Kasahara[a,3]

[a]Department of Pathology, Hokkaido University Graduate School of Medicine, 060-8638 Sapporo, Japan; and [b]Division of Immunobiology, Institute for Genetic Medicine, Hokkaido University, 060-0815 Sapporo, Japan

Edited* by Max D. Cooper, Emory University, Atlanta, GA, and approved July 9, 2010 (received for review February 18, 2010)

Jawless vertebrates such as lamprey and hagfish lack T-cell and B-cell receptors; instead, they have unique antigen receptors known as variable lymphocyte receptors (VLRs). VLRs generate diversity by recombining highly diverse leucine-rich repeat modules and are expressed clonally on lymphocyte-like cells (LLCs). Thus far, two types of receptors, VLRA and VLRB, have been identified in lampreys and hagfish. Recent evidence indicates that VLRA and VLRB are expressed on distinct populations of LLCs that resemble T cells and B cells of jawed vertebrates, respectively. Here we identified a third VLR, designated VLRC, in the lamprey. None of the ≈100 VLRC cDNA clones subjected to sequencing had an identical sequence, indicating that *VLRC* can generate sufficient diversity to function as antigen receptors. Notably, the C-terminal cap of VLRC exhibits only limited diversity and has important structural differences relative to VLRA and VLRB. Single-cell PCR analysis identified LLCs that rearranged *VLRC* but not *VLRA* or *VLRB*, suggesting the presence of a unique population of LLCs that express only VLRC.

antigen receptors | immune system evolution | jawless vertebrates | leucine-rich repeats | somatic rearrangement

Jawless vertebrates such as lamprey and hagfish produce specific agglutinins when immunized with particulate antigens (1–7). Hence, they were long thought to have immunoglobulins. Accumulated evidence indicates, however, that jawless vertebrates have neither immunoglobulins nor T cell receptors but instead have unique antigen receptors called variable lymphocyte receptors (VLRs) (8–15). Whereas immunoglobulins and T cell receptors generate repertoire diversity by recombining variable (V), diversity (D), and joining (J) gene segments, VLRs achieve comparable diversity through the rearrangement of highly diverse leucine-rich repeat (LRR) modules (16, 17). The germline *VLR* gene has an incomplete structure incapable of encoding functional proteins; it is, however, flanked by a large number of LRR-encoding modules exhibiting remarkable sequence diversity. During the development of lymphocyte-like cells (LLCs), these modules are incorporated into the *VLR* gene by a gene conversion-like process presumably mediated by cytidine deaminases of the AID-APOBEC family (18–20). Crystallographic analysis of VLR monomers showed that they adopt a horseshoe-shaped structure and suggested that they most likely bind antigens through the hypervariable concave surface composed of β-strands (21). This suggestion was confirmed recently by in vitro mutagenesis experiments (22) and the crystal structure analysis of VLR monomer–antigen complexes (23, 24).

Two *VLR* genes, designated *VLRA* and *VLRB*, have been identified in hagfish and lampreys (19, 25, 26). In hagfish, *VLRA* and *VLRB* are encoded by two separate loci (27), suggesting that the two *VLR* genes function as independent recombination units; the same seems to be the case with the lamprey genes (19). Surprisingly, recent evidence indicates that lamprey VLRA and VLRB are expressed on distinct populations of LLCs that resemble T cells and B cells of jawed vertebrates, respectively (28). When challenged with antigen, LLCs expressing specific VLRB molecules undergo blast transformation, expand clonally, and begin to secrete VLRB molecules in a manner analogous to the secretion of immunoglobulins by B cells (29). Secreted VLRB molecules, which form pentamers or tetramers of dimers (22), function as strong agglutinins, thus accounting for the earlier observations suggesting the existence of antibodies in jawless vertebrates (1–7). By contrast, VLRA molecules are expressed on a population of $VLRB^-$ LLCs and apparently occur only in a membrane-bound form; this population of LLCs responds to a T cell mitogen and up-regulates the expression of interleukin-17 (28), indicating that lampreys have humoral and cellular arms of adaptive immunity analogous to those of jawed vertebrates.

Here we analyzed publicly available sea lamprey (*Petromyzon marinus*) EST sequences and identified a previously undescribed *VLR* gene, which we propose to call *VLRC*.

Results

Identification of the *VLRC* Gene. We collected sea lamprey EST sequences from the National Center for Biotechnology Information (NCBI) trace archive and constructed an EST database. TBLASTN searches of this database using hagfish VLRA and VLRB (accession nos. ABB59067 and ABB59026, respectively) as query proteins identified an EST clone that predicted a VLR-like protein with a 3′ terminus distinct from those of known VLRs.

To establish the identity of this clone (accession no. EC382912.1), we isolated the corresponding cDNA fragment from the Japanese lamprey (*Lethenteron japonicum*) by 3′-RACE. The Japanese lamprey leukocyte cDNA library was then screened using this fragment as a probe. We chose a cDNA clone that seemed to contain a full-length insert and determined its complete sequence (accession no. AB507271). This clone encoded a protein consisting of a 24-residue signal peptide (SP), 36-residue N-terminal cap (LRRNT), 25-residue LRR1, 24-residue LRR, 24-residue LRRVe, 16-residue connecting peptide (CP), 49-residue C-terminal cap (LRRCT), and 74-residue 3′ terminus (Fig. 1). The top 50 BLAST hits to this protein were all agnathan VLRs, with inshore hagfish (*Eptatretus burgeri*) VLRA encoded by clone Es6VLRA.H5 showing the greatest similarity (49% amino acid identity). The SP and 3′ terminus of this protein were, however, only weakly similar to those of known sea lamprey VLRs, suggesting that it is a unique member of the VLR family. Isolation of Japanese lamprey VLRA and VLRB cDNAs confirmed the existence of three types of VLRs in a single lamprey species (Fig. 1). Therefore, the VLR identified in this study was named VLRC. In all known VLRs, LRRNT and LRRCT contain a characteristic four-cysteine motif CX_nCXCX_nC

Author contributions: J.K., Y.S., and M.K. designed research; J.K., Y.S., K.F., N.O., and K.I. performed research; J.K., Y.S., K.I., and M.K. analyzed data; and J.K., Y.S., and M.K. wrote the paper.

The authors declare no conflict of interest.

*This Direct Submission article had a prearranged editor.

Data deposition: The sequences reported in this paper have been deposited in the GenBank database (accession nos. AB507269–AB507373).

[1]J.K. and Y.S. contributed equally to this work.

[2]Present address: Department of Microbiology and Immunology, Hokkaido University Graduate School of Medicine, 060-8638 Sapporo, Japan.

[3]To whom correspondence should be addressed. E-mail: mkasaha@med.hokudai.ac.jp.

This article contains supporting information online at www.pnas.org/lookup/suppl/doi:10.1073/pnas.1001910107/-/DCSupplemental.

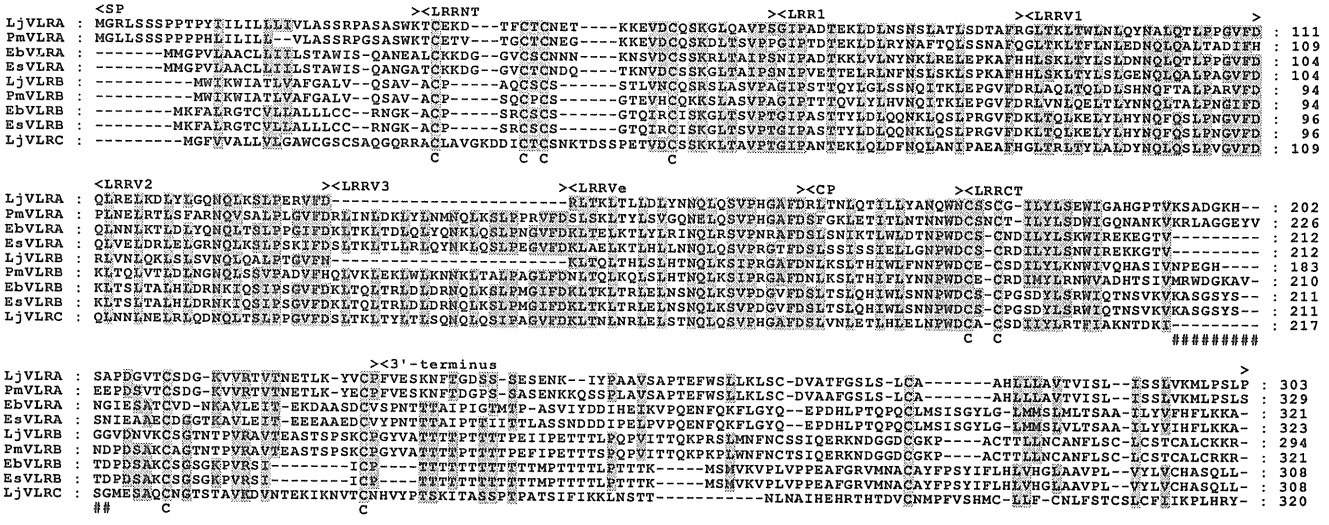

Fig. 1. VLRC is a member of the VLR family. Deduced amino acid sequences of sea lamprey (Pm, *P. marinus*), Japanese lamprey (Lj, *L. japonicum*), inshore hagfish (Eb, *E. burgeri*), and Pacific hagfish (Es, *Eptatretus stoutii*) VLRs. C, conserved cysteine residues in LRRNT and LRRCT; #, highly variable inserts (23). Conserved residues are shaded: light-blue, ≥90% identity; green, 70–89% identity; and yellow, 69–50% identity. "-" indicates a gap. Accession nos. are as follows: LjVLRA, AB507269; PmVLRA, EF094821; EbVLRA, AY964726; EsVLRA, AY964825; LjVLRB, AB507270; PmVLRB, AY577957; EbVLRB, AY965530; EsVLRB, AY965561; and LjVLRC, AB507271.

(where X stands for any amino acid other than cysteine). These motifs, known to be involved in the formation of two sets of disulfide bridges, are also present in VLRC.

We constructed 3D models of VLRC and VLRA using the crystal structure of lamprey VLRB specific for the H-trisaccharide of human blood group O antigen (23) as a template (Fig. S1). VLRC was predicted to have a structure similar to that of lamprey VLRB but to lack protrusions located in the LRRCT of VLRB. By contrast, the LRRCT of some lamprey VLRA molecules was predicted to form a protrusion.

Germline Structure of the *VLRC* Locus. To determine the germline structure of the *VLRC* gene, Japanese lamprey genomic DNA was subjected to PCR using a set of primers designed to amplify the region spanning from 5′-UTR to 3′-UTR. Only a single DNA fragment of 1,154 bp was obtained, indicating that *VLRC* is a single-copy gene. This fragment was sequenced completely (accession no. AB507272) and its sequence compared with the full-length *VLRC* cDNA sequence. Like other *VLR* genes, the germline *VLRC* gene lacks sequences coding for LRR modules and contains only the sequences coding for 5′-UTR, SP, LRRNT, 5′-part of LRR1, 3′-part of CP, LRRCT, 3′ terminus, and 3′-UTR (Fig. 2*A*); 5′-part of LRR1 and 3′-part of CP are separated by a sequence of 161 bp with no apparent similarity to any known sequence. Similar to other *VLR* genes, *VLRC* contained an intron (35 bp) in its 5′-UTR.

Analysis of the sea lamprey genome assembly revealed that this lamprey species also has a single copy of *VLRC* and that the organization of the germline *VLRC* gene is conserved between the two lamprey species. Two 5′-LRRCT-encoding modules, designated modules 1 and 2, respectively, were identified downstream of the *VLRC* gene (Fig. 2*B*). BLAST searches of the sea lamprey genome identified no other 5′-LRRCT-encoding modules with significant similarity to those observed in Japanese lamprey *VLRC* transcripts. Among known *VLR* genes, the structure of germline *VLRC* is unique in that it contains LRRNT- and LRRCT-modules in their entirety (Fig. 2*A*).

***VLRC* Generates Diversity Comparable to That of *VLRA* and *VLRB*, but Its LRRCT Shows Only Limited Diversity.** To assess the extent of diversity generated by the *VLRC* gene, we cloned the region spanning from LRRNT to LRRCT by RT-PCR from the leukocytes of five Japanese lampreys and sequenced a total of 101 clones (Fig. S2). None of the clones had an identical nucleotide sequence, and the number of 24-residue LRR modules varied from zero to four. Of the 302 LRR modules encoded by these clones, 70% had unique sequences. Similarly, 66% of LRR1, 53% of CP, and 75% of LRRVe had unique sequences. These figures are comparable to those previously reported for hagfish VLRA (25), hagfish VLRB (25), lamprey VLRB (17), and lamprey VLRA molecules (19). Thus, *VLRC* seems to be capable of generating diversity comparable to that of *VLRA* and *VLRB*.

Consistent with the observation that LRRCT is involved in antigen recognition (23, 24), the 5′-LRRCT of lamprey VLRA and VLRB exhibits high levels of sequence diversity. By contrast, only two major types of 5′-LRRCT sequences were detected in Japanese lamprey VLRC (Fig. 2*C* and Fig. S2). One type completely or closely matched the 5′-LRRCT sequence encoded by the germline *VLRC* gene; another type fell into two closely related subtypes, with sequences almost identical to those of modules 1 and 2 located downstream of the sea lamprey *VLRC* gene, respectively (Fig. 2*C*). These observations suggest that, similar to sea lampreys, Japanese lampreys have 5′-LRRCT-encoding modules corresponding to modules 1 and 2 and that they use such modules for *VLRC* assembly, along with the 5′-LRRCT module encoded by the germline gene. The 5′-LRRCT sequence encoded by the germline gene was so divergent from that encoded by module 1 or 2 that VLRC clones formed distinct clusters (Fig. S3) depending on whether their 5′-LRRCTs were derived from the germline gene (marked with filled circles) or from module 1 or 2 (marked with open circles).

Phylogenetic Analysis Indicates That VLRC Is More Closely Related to VLRA Than to VLRB. To examine the relationship of VLRC to known VLRs, we constructed a neighbor-joining tree (Fig. 3). The tree supported the orthologous relationship of hagfish and lamprey VLRB and showed that VLRC is more closely related to hagfish and lamprey VLRA than to hagfish and lamprey VLRB. Lamprey VLRA and VLRC were almost equidistant from hagfish VLRA, and their relationship could not be resolved with high bootstrap support, thus precluding us to determine

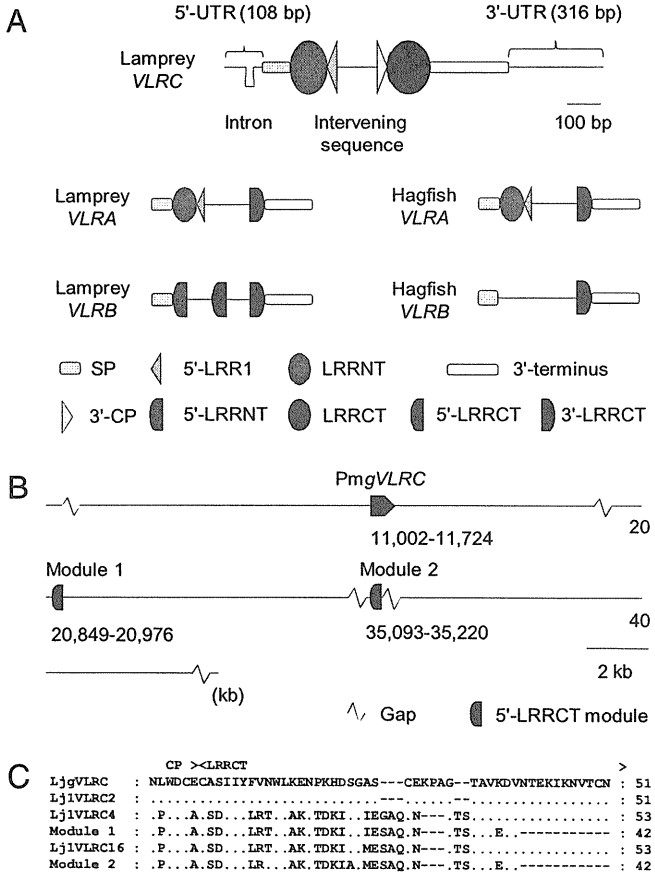

Fig. 2. Organization of the germline *VLRC* locus. (*A*) Structure of the germline *VLRC* gene of the Japanese lamprey (drawn to scale) and the schematic germline structures of other known *VLR* genes (not drawn to scale). (*B*) Organization of the sea lamprey *VLRC* locus. Two 5′-LRRCT-encoding modules, designated modules 1 and 2, are located downstream of the germline *VLRC* gene. This information is based on the analysis of contig 377 in the Pre Ensembl genome database. (*C*) The 5′-LRRCT of VLRC shows only limited diversity; basically only two major types of sequences were observed. One type represented by Lj1VLRC2 has a sequence identical or nearly identical to the 5′-LRRCT sequence located in the germline *VLRC* gene (LjgVLRC). The other type falls into two closely related subtypes represented by Lj1VLRC4 and Lj1VLRC16; the sequences of these clones are very similar to those of modules 1 and 2, respectively. "." and "-" indicate identity with the top sequence and absence of residues, respectively. Clones are identified by the species name, followed by the animal number, gene name, and clone number. Thus, Lj1VLRC2 indicates a VLRC clone 2 isolated from Japanese lamprey individual 1.

which lamprey gene is orthologous to hagfish *VLRA* according to sequence comparison alone.

Identification of a Unique Population of LLCs That Rearrange Only the *VLRC* Gene. We compared by RT-PCR the expression profiles of *VLRA*, *VLRB*, and *VLRC* in representative tissues of adult lampreys using elongation factor 1α (EF1α) as a positive control (Fig. 4*A*). The three *VLR* genes showed similar expression patterns, with transcripts detected most abundantly in peripheral blood leukocytes, followed by gills, intestine, and kidney. Real-time RT-PCR analysis showed that *VLRC* transcripts were ≈60–100 times less abundant than *VLRB* transcripts in all of the tissues examined; on the other hand, the expression levels of *VLRC* and *VLRA* were nearly the same (Fig. 4*B*).

To examine whether VLRC$^+$ cells are distinct from those expressing known VLRs, we generated mAbs specific for VLRA and VLRB, respectively. The specificities of these mAbs were verified by testing against a panel of transfected mammalian cells

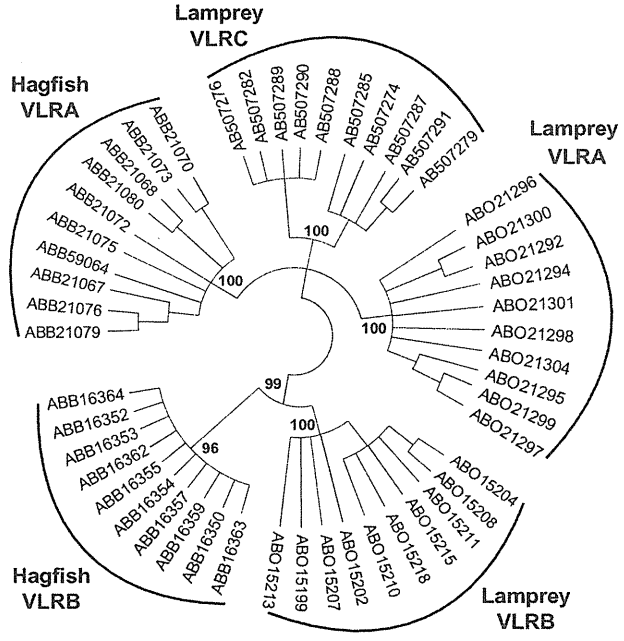

Fig. 3. Phylogenetic relationship of *VLR* genes. A neighbor-joining tree was constructed using the amino acid sequences of the diversity region that could be reliably aligned (LRRNT, LRR1, LRRVe, and LRRCT). Nodes that received bootstrap support of <70% were collapsed. Bootstrap values >90% are shown. For abbreviations of species' names, see the legend to Fig. 1.

expressing VLRA, VLRB, or VLRC (Fig. S4). Purified LLCs (≈92% LLCs as judged by forward and side scatter characteristics and Giemsa staining) were subjected to magnetic cell sorting with VLRB-specific mAb, and then the flow-through was flow-sorted into VLRA$^+$ and VLRA$^-$/VLRB$^-$ fractions. The latter fraction was assumed to contain VLRC$^+$ cells. Each of the three fractions, VLRA$^+$, VLRB$^+$, and VLRA$^-$/VLRB$^-$, was subjected to single-cell sorting, and rearrangements of *VLR* genes were assessed by genomic PCR. Representative electrophoretic profiles of single-cell PCR products are shown for VLRA$^+$, VLRB$^+$, and VLRA$^-$/VLRB$^-$ cells (Fig. 5). We typically observed a germline product along with a rearranged product. Of 24 VLRA$^-$/VLRB$^-$ cells in which *VLRC* assembly was detected, 23 cells rearranged the *VLRC* gene and maintained the *VLRA* and *VLRB* genes in germline configuration, indicating the existence of a unique population of LLCs that exclusively express *VLRC*. In one cell, we detected assembly of both *VLRA* and *VLRC* genes; however, consistent with the VLRA$^-$ phenotype, the rearranged *VLRA* gene contained a 2-bp insertion in its diversity region, resulting in a frameshift mutation. Thus, only the rearranged *VLRC* gene was apparently functional in this cell.

Discussion

The *VLRC* gene described here generates diversity comparable to that of *VLRA* and *VLRB* by rearranging highly diverse LRR modules (Figs. S2 and S3); the rearranged *VLRC* gene is transcribed predominantly in peripheral blood leukocytes and tissues thought to be involved in hematopoiesis (kidney and intestine) or defenses at the body surface (gill and intestine) (Fig. 4). Furthermore, single-cell PCR experiments provided convincing evidence for the presence of LLCs in which only the *VLRC* gene is rearranged (Fig. 5). Collectively, these observations indicate the existence of a unique population of LLCs that solely express VLRC as antigen receptors. Thus, lampreys have at least three populations of LLCs distinguished by differential expression of the three *VLR* loci.

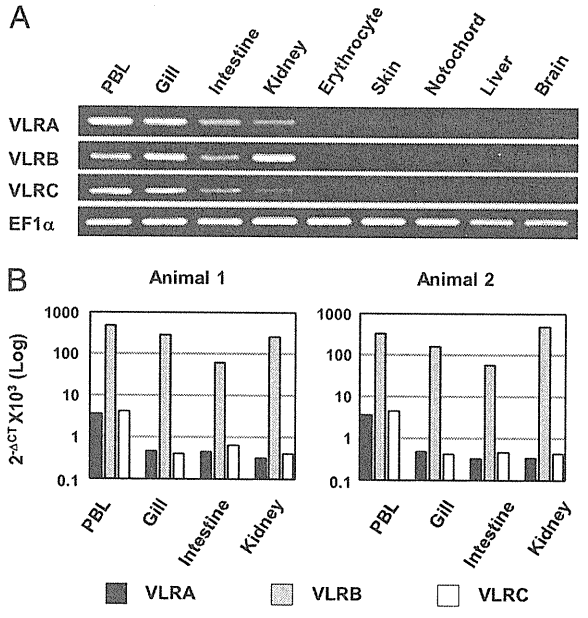

Fig. 4. Tissue distribution of *VLRC* transcripts in Japanese lampreys. (*A*) Tissue distribution of *VLRA*, *VLRB*, and *VLRC* transcripts. PBL, peripheral blood leukocytes. (*B*) Real-time RT-PCR analysis. Two animals were subjected to experiments.

The 5′-LRRCT region exhibits high levels of sequence diversity in VLRA and VLRB molecules; consistent with this, the sea lamprey genome contains 54 and 58 5′-LRRCT-encoding modules that can potentially be used for *VLRA* and *VLRB* assembly, respectively (16, 19). By contrast, besides the module encoded by the germline gene, the lamprey genome seems to contain only two 5′-LRRCT–encoding modules used for *VLRC* assembly (Fig. 2*A*). Consequently, the 5′-LRRCT region of VLRC shows only limited diversity (Fig. 2*C* and Fig. S2). This observation may have functional significance because, in VLRB molecules, 5′-LRRCT is known to be involved in antigen recognition (23, 24). If the same is the case with VLRC, VLRC might recognize antigens bearing conserved epitopes or antigens in association with invariant molecules, with its LRRCT and LRR interacting with conserved and variable epitopes, respectively.

Another notable feature of VLRC is that, unlike lamprey VLRA or VLRB, its 5′-LRRCT is predicted to lack the capacity to form protrusions (Fig. S1). In lamprey VLRB molecules, these protrusions are formed by a stretch of amino acid residues, known as a highly variable insert, that displays marked variations in length, amino acid composition, and secondary structure (23). In a VLRB molecule, RBC36, a 10-residue insert forms a β-hairpin protrusion that interacts with H-antigen trisaccharide (23). In another VLRB molecule, VLRB.2D, a six-residue insert forms a protrusion that extends to the catalytic cleft of hen egg lysozyme (24). Consistent with the observation that lamprey VLRA molecules have a variable insert with the average length of 12 residues (24), 3D modeling predicted protrusions in some VLRA molecules (Fig. S1). By contrast, the region of VLRC corresponding to the variable insert contains only a few residues (Fig. 1 and Fig. S2) and hence is too short to form any protrusions. This structural feature might impose additional restrictions on the nature of antigen recognized by VLRC.

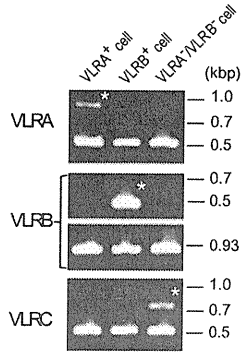

Fig. 5. Identification of LLCs that rearrange only the *VLRC* gene. Single-cell genomic PCR identified LLCs that rearranged only the *VLRA* (*Left*), *VLRB* (*Center*), or *VLRC* (*Right*) gene. Bands marked with asterisks represent rearranged products, whereas unmarked bands represent germline products.

Phylogenetically, *VLRB* is present in both hagfish and lampreys, and *VLRC* is more closely related to *VLRA* than to *VLRB* (Fig. 3). This observation indicates that, in a common ancestor of hagfish and lampreys, a primordial *VLR* gene duplicated to give rise to *VLRB* and a common ancestor of *VLRA* and *VLRC*, and that this was followed by a second duplication event that separated *VLRA* from *VLRC*. The observation that lamprey *VLRA* and *VLRC* are almost equally related to hagfish *VLRA* (Fig. 3) raises three major possibilities concerning their relationship. First, lamprey *VLRA* is orthologous to hagfish *VLRA*, and hagfish *VLRC* remains to be identified. Second, lamprey *VLRC* is orthologous to hagfish *VLRA*, and the lamprey counterpart of hagfish *VLRA* remains to be identified. Third, lamprey *VLRA* and *VLRC* diverged in a lamprey lineage soon after its separation from a hagfish lineage, and thus, neither lamprey *VLRA* nor *VLRC* is orthologous to hagfish *VLRA*. The germline *VLRA* genes of hagfish and lamprey have an identical structure, whereas the germline structure of lamprey *VLRC* is unique (Fig. 2*A*). This observation argues against the second possibility because gene structure is generally more conserved than protein sequences during evolution. Thus, the first and third possibilities remain open at the moment.

Despite the fact that VLRs are structurally unrelated to T/B cell receptors, both receptors rely on combinatorial diversity to generate a vast repertoire of binding specificities, highlighting similarities in immune defense strategies adopted by all vertebrates. Most remarkable in this regard is the recent demonstration that cells expressing VLRA and VLRB resemble T cells and B cells of jawed vertebrates, respectively (28). This naturally raises the question, "Do $VLRC^+$ cells resemble T cells or B cells?" Previous work has shown that lamprey agglutinins generated against human erythrocytes are exclusively derived from $VLRB^+$ cells (29). Together with our observation that VLRC is phylogenetically more closely related to VLRA (Fig. 3), this finding suggests that $VLRC^+$ cells probably resemble T cells rather than B cells. If $VLRC^+$ cells are indeed T cell-like, another interesting question arises: "Are $VLRA^+$ and $VLRC^+$ cells functionally specialized in a manner analogous to αβ and γδ T cells of jawed vertebrates?" The discovery of VLRC provides an opportunity to further examine the origin of lymphocytes and the similarities and dissimilarities of host defense strategies used by jawed and jawless vertebrates.

Materials and Methods

Animals. Adult Japanese lampreys were purchased from local dealers and maintained in temperature-controlled tanks. All procedures of animal experimentation were approved by the Institutional Review Board of Hokkaido University.

Computational Analysis. Sea lamprey EST sequences were retrieved from the NCBI trace archive (http://www.ncbi.nlm.nih.gov/Traces/trace.cgi), and a private database was constructed with the GENETYX-PDB program package (version 5; GENETYX). This database was searched with the TBLASTN program implemented in the package. The genomic organization of the sea lamprey *VLRC* gene was determined using the Pre Ensembl genome browser (http://pre.ensembl.org/Petromyzon_marinus/Info/Index). 3D models of lamprey

IMMUNOLOGY

VLRA and VLRC were generated using the SWISS-MODEL server (30) and edited by PyMol (http://pymol.sourceforge.net).

Isolation of Japanese Lamprey VLR cDNA and Genomic Clones. Partial cDNA fragments coding for Japanese lamprey VLRA, VLRB, and VLRC were obtained by RACE using the primers designed in the regions predicted to be conserved between sea lampreys and Japanese lampreys. The cDNA fragments thus obtained were used as probes to screen a λZAPII cDNA library constructed from Japanese lamprey leukocytes, which resulted in the isolation of full-length VLRB and VLRC cDNA clones. Full-length VLRA cDNA clones were isolated by 5′- and 3′-RACE. The genomic clone containing germline *VLRC* was isolated by PCR using Japanese lamprey genomic DNA as a template (primer sequences: 5′-TGGTCCCGTGCGAGCCGAGCC-3′ and 5′-CGCTATGCAACGGGGATGTCTAC-3′).

Phylogenetic Analysis. Amino acid sequences were aligned with the Clustal X version 2 program (31). The distance matrix was obtained by calculating Poisson-correction distances for all pairs of sequences. Sites containing gaps were excluded from the analysis using the pairwise deletion option. Neighbor-joining trees were constructed using the MEGA version 4 program (32). The reliability of branching patterns was assessed by bootstrap analysis (500 replications).

Expression Analysis. Tissue expression profiles of *VLR* genes were analyzed by conventional and real-time RT-PCR using the same primer sets. The primer sequences for *VLRA*, *VLRB*, *VLRC*, and a reference housekeeping gene *EF1A* were 5′-ACCGTGAAGAGAGAGGATTGT-3′ and 5′-CTTTTCACACGTTTTCCACGA-3′, 5′-CAGCTACAGCCACCACTGTCT-3′ and 5′-GGGACATGCTACTGCACTTT-3′, 5′-TTCATCATTCTGAAGATTATCGCTG-3′ and 5′-TTGCCGACCGCAAGGCAAGCT-3′, and 5′-GTCTACAAAATTGGCGGTATT-3′ and 5′-ACATCCTTGACAGACACGTT-3′, respectively. Cycling conditions were 1 cycle at 95 °C for 10 min, followed by 30 or 35 cycles of denaturation at 95 °C for 15 s and annealing/extension at 60 °C for 1 min (30 cycles for *VLRB* and *EF1A*, 35 cycles for *VLRA* and *VLRC*). Real-time PCR was conducted as previously described (33) using an ABI PRISM 7000 sequence detection system (Applied Biosystems).

Magnetic Cell Sorting. Whole blood isolated from lampreys was suspended in 60% PBS containing 100 mM EDTA and centrifuged for 5 min at 500 × *g*. The pellet was resuspended in the same solution and centrifuged for 5 min at 220 × *g*. Cells in the supernatant were collected and further purified with Histopaque-1077 (Sigma-Aldrich) to obtain LLCs. Magnetic cell sorting was performed using MACS anti-PE MicroBeads according to the instructions of the manufacturer (Miltenyi Biotec). Briefly, 1×10^7 LLCs were reacted with mAb specific for VLRB at 4 °C for 15 min. After washing, they were reacted with 1:10-diluted PE-conjugated anti-mouse IgG $F(ab')_2$ fragment (eBioscience) at 4 °C for 15 min. They were then washed with buffer, mixed with anti-PE MicroBeads, and applied to the MACS MS columns.

Single-Cell Genomic PCR. LLCs were sorted and seeded at one cell per well into 96-well plates using BD FACSAria II. Each well was preloaded with 10 μL of LA-Taq PCR buffer (TaKaRa). Single-cell genomic PCR was performed as described previously (18, 20). The primer sets for *VLRA* were 5′-ATTGTGCATCCAC-AGCCACT-3′ and 5′-ATCTTGACGAGGCTGGAGAT-3′ for multiplex PCR and 5′-CCTCATCGGTGCAGATCAC-3′ and 5′-CTCACTGCCGCAGGATAAAT-3′ for nested PCR. Those for *VLRC* were 5′-TGGTCCCGTGCGAGCCGAGCC-3′ and 5′-CGTTCT-GTGCTCATGGATTG-3′ for multiplex PCR and 5′-ATGGGGTTTGTCGTGGCGCT-3′ and 5′-TTGCATTGAGATTGGTGGTC-3′ for nested PCR. The primer sets for *VLRB* were described previously (18, 20).

ACKNOWLEDGMENTS. We thank Dr. Satoshi Kusuda (Hokkaido Fish Hatchery) for his help in procuring lampreys and Dr. Fumikiyo Nagawa (University of Tokyo) for his advice on single-cell PCR. This work was supported by Grants-in-Aids from The Ministry of Education, Culture, Sports, Science and Technology of Japan and by grants from the Japan Science and Technology Agency and the NOASTEC Foundation. J.K. and Y.S. were supported by the Research Fellowship for Young Scientists from the Japan Society for the Promotion of Science.

1. Finstad J, Good RA (1964) The evolution of the immune response. III. Immunologic responses in the lamprey. *J Exp Med* 120:1151–1168.
2. Boffa GA, Fine JM, Drilhon A, Amouch P (1967) Immunoglobulins and transferrin in marine lamprey sera. *Nature* 214:700–702.
3. Marchalonis JJ, Edelman GM (1968) Phylogenetic origins of antibody structure. 3. Antibodies in the primary immune response of the sea lamprey, *Petromyzon marinus*. *J Exp Med* 127:891–914.
4. Linthicum DS, Hildemann WH (1970) Immunologic responses of Pacific hagfish. 3. Serum antibodies to cellular antigens. *J Immunol* 105:912–918.
5. Pollara B, Litman GW, Finstad J, Howell J, Good RA (1970) The evolution of the immune response. VII. Antibody to human "O" cells and properties of the immunoglobulin in lamprey. *J Immunol* 105:738–745.
6. Litman GW, Finstad FJ, Howell J, Pollara BW, God RA (1970) The evolution of the immune response. 3. Structural studies of the lamprey immuoglobulin. *J Immunol* 105:1278–1285.
7. Fujii T, Nakagawa H, Murakawa S (1979) Immunity in lamprey. II. Antigen-binding responses to sheep erythrocytes and hapten in the ammocoete. *Dev Comp Immunol* 3: 609–620.
8. Litman GW, Cannon JP, Dishaw LJ (2005) Reconstructing immune phylogeny: New perspectives. *Nat Rev Immunol* 5:866–879.
9. Pancer Z, Cooper MD (2006) The evolution of adaptive immunity. *Annu Rev Immunol* 24:497–518.
10. Cooper MD, Alder MN (2006) The evolution of adaptive immune systems. *Cell* 124: 815–822.
11. Kasahara M, Kasamatsu J, Sutoh Y (2008) Two types of antigen receptor systems in vertebrates. *Zoolog Sci* 25:969–975.
12. Flajnik MF, Du Pasquier L (2008) *Fundamental Immunology*, ed Paul WE (Lippincott Williams & Wilkins, Philadelphia), pp 56–124.
13. Cooper MD, Herrin BR (2010) How did our complex immune system evolve? *Nat Rev Immunol* 10:2–3.
14. Flajnik MF, Kasahara M (2010) Origin and evolution of the adaptive immune system: Genetic events and selective pressures. *Nat Rev Genet* 11:47–59.
15. Boehm T (2009) One problem, two solutions. *Nat Immunol* 10:811–813.
16. Pancer Z, et al. (2004) Somatic diversification of variable lymphocyte receptors in the agnathan sea lamprey. *Nature* 430:174–180.
17. Alder MN, et al. (2005) Diversity and function of adaptive immune receptors in a jawless vertebrate. *Science* 310:1970–1973.
18. Nagawa F, et al. (2007) Antigen-receptor genes of the agnathan lamprey are assembled by a process involving copy choice. *Nat Immunol* 8:206–213.
19. Rogozin IB, et al. (2007) Evolution and diversification of lamprey antigen receptors: Evidence for involvement of an AID-APOBEC family cytosine deaminase. *Nat Immunol* 8:647–656.
20. Kishishita N, et al. (2010) Regulation of antigen-receptor gene assembly in hagfish. *EMBO Rep* 11:126–132.
21. Kim HM, et al. (2007) Structural diversity of the hagfish variable lymphocyte receptors. *J Biol Chem* 282:6726–6732.
22. Herrin BR, et al. (2008) Structure and specificity of lamprey monoclonal antibodies. *Proc Natl Acad Sci USA* 105:2040–2045.
23. Han BW, Herrin BR, Cooper MD, Wilson IA (2008) Antigen recognition by variable lymphocyte receptors. *Science* 321:1834–1837.
24. Velikovsky CA, et al. (2009) Structure of a lamprey variable lymphocyte receptor in complex with a protein antigen. *Nat Struct Mol Biol* 16:725–730.
25. Pancer Z, et al. (2005) Variable lymphocyte receptors in hagfish. *Proc Natl Acad Sci USA* 102:9224–9229.
26. Tasumi S, et al. (2009) High-affinity lamprey VLRA and VLRB monoclonal antibodies. *Proc Natl Acad Sci USA* 106:12891–12896.
27. Kasamatsu J, Suzuki T, Ishijima J, Matsuda Y, Kasahara M (2007) Two variable lymphocyte receptor genes of the inshore hagfish are located far apart on the same chromosome. *Immunogenetics* 59:329–331.
28. Guo P, et al. (2009) Dual nature of the adaptive immune system in lampreys. *Nature* 459:796–801.
29. Alder MN, et al. (2008) Antibody responses of variable lymphocyte receptors in the lamprey. *Nat Immunol* 9:319–327.
30. Arnold K, Bordoli L, Kopp J, Schwede T (2006) The SWISS-MODEL workspace: A web-based environment for protein structure homology modelling. *Bioinformatics* 22: 195–201.
31. Larkin MA, et al. (2007) Clustal W and Clustal X version 2.0. *Bioinformatics* 23: 2947–2948.
32. Kumar S, Nei M, Dudley J, Tamura K (2008) MEGA: A biologist-centric software for evolutionary analysis of DNA and protein sequences. *Brief Bioinform* 9:299–306.
33. Suzuki T, Shin-I T, Fujiyama A, Kohara Y, Kasahara M (2005) Hagfish leukocytes express a paired receptor family with a variable domain resembling those of antigen receptors. *J Immunol* 174:2885–2891.

Published November 8, 2010

JEM

Article

Identification of a polyI:C-inducible membrane protein that participates in dendritic cell–mediated natural killer cell activation

Takashi Ebihara,[1] Masahiro Azuma,[1] Hiroyuki Oshiumi,[1] Jun Kasamatsu,[1] Kazuya Iwabuchi,[2] Kenji Matsumoto,[3] Hirohisa Saito,[3] Tadatsugu Taniguchi,[4] Misako Matsumoto,[1] and Tsukasa Seya[1]

[1]Department of Microbiology and Immunology, Hokkaido University Graduate School of Medicine, Kita-ku, Sapporo 060-8638, Japan
[2]Division of Immunobiology, Institute for Genetic Medicine, Hokkaido University, Sapporo, Japan, 060-0815, Japan
[3]Department of Allergy and Immunology, National Research Institute for Child Health and Development, Setagaya-ku, Tokyo 157-8535, Japan
[4]Department of Immunology, Graduate School of Medicine and Faculty of Medicine, University of Tokyo, Bunkyo-ku, Tokyo 113-0033, Japan

In myeloid dendritic cells (mDCs), TLR3 is expressed in the endosomal membrane and interacts with the adaptor toll/interleukin 1 receptor homology domain–containing adaptor molecule 1 (TICAM-1; TRIF). TICAM-1 signals culminate in interferon (IFN) regulatory factor (IRF) 3 activation. Co-culture of mDC pretreated with the TLR3 ligand polyI:C and natural killer (NK) cells resulted in NK cell activation. This activation was triggered by cell-to-cell contact but not cytokines. Using expression profiling and gain/loss-of-function analyses of mDC genes, we tried to identify a TICAM-1–inducing membrane protein that participates in mDC-mediated NK activation. Of the nine candidates screened, one contained a tetraspanin-like sequence and satisfied the screening criteria. The protein, referred to as IRF-3–dependent NK-activating molecule (INAM), functioned in both the mDC and NK cell to facilitate NK activation. In the mDC, TICAM-1, IFN promoter stimulator 1, and IRF-3, but not IRF-7, were required for mDC-mediated NK activation. INAM was minimally expressed on NK cells, was up-regulated in response to polyI:C, and contributed to mDC–NK reciprocal activation via its cytoplasmic tail, which was crucial for the activation signal in NK cells. Adoptive transfer of INAM-expressing mDCs into mice implanted with NK-sensitive tumors caused NK-mediated tumor regression. We identify a new pathway for mDC–NK contact-mediated NK activation that is governed by a TLR signal–derived membrane molecule.

CORRESPONDENCE
Tsukasa Seya:
seya-tu@pop.med.hokudai.ac.jp

Abbreviations used: BMDC, BM-derived DC; IKK, IκB kinase; INAM, IRF-3–dependent NK-activating molecule; IPS-1, IFN promoter stimulator 1; IRF, IFN regulatory factor; mDC, myeloid DC; PRR, pattern recognition receptor; Rae-1, retinoic acid–inducible gene 1; TICAM-1, toll/IL-1 receptor homology domain–containing adaptor molecule 1; TLR, Toll-like receptor.

Natural killer (NK) cells contribute to innate immune responses by killing virus-infected or malignantly transformed cells and by producing cytokines such as IFN-γ and TNF. NK cell activation is determined by a balance of signals from inhibitory and activating receptors. Because ligands of inhibitory receptors include MHC class I and class I–like molecules, the absence of self-MHC expression leads to NK activation (Cerwenka and Lanier, 2001). Approximately 20 receptors contribute to NK activation (Cerwenka and Lanier, 2001; Vivier et al., 2008). When ligands for activating receptors are sufficiently abundant, activating signals overcome inhibitory signals.

There are two currently accepted models for in vivo NK activation. One is that NK cells usually circulate in a naive state and are activated through interaction directly with ligands for pattern recognition receptors (PRRs) expressed by NK cells or interaction with cells that express PRR ligands (Hornung et al., 2002; Sivori et al., 2004). When pathogens enter the host, innate immune sensors, such as Toll-like receptors (TLRs), RIG-I-like receptors,

T. Ebihara and M. Azuma contributed equally to this paper.
T. Ebihara's present address is Howard Hughes Medical Institute, Washington University School of Medicine, St. Louis, MO 63110.

The Rockefeller University Press $30.00
J. Exp. Med. Vol. 207 No. 12 2675-2687
www.jem.org/cgi/doi/10.1084/jem.20091573

Supplemental Material can be found at:
http://jem.rupress.org/content/suppl/2010/11/04/jem.20091573.DC1.html

Published November 8, 2010

NOD-like receptors, and lectin family proteins, which are PRRs, recognize a variety of microbial patterns (pathogen-associated molecular patterns [PAMPs]; Medzhitov and Janeway, 1997). Mouse NK cells express almost all TLRs (TLR1–3, 4, and 6–9), and some of these are directly activated by pathogens with the help of IL-12, IL-18, IFN-γ, and other cytokines (Newman and Riley, 2007). The other is that naive NK cells tend to be recruited to the draining LNs, where they are primed to be effectors with the help of mature myeloid DCs (mDC) and released into peripheral tissues (Fernandez et al., 1999). In this case, mDCs provide direct activating signals to NK cells through cell–cell contact (Gerosa et al., 2002; Akazawa et al., 2007a; Lucas et al., 2007). mDCs also produce proinflammatory cytokines and IFN-α after recognizing PAMPs (Newman and Riley, 2007). In this mDC-mediated NK activation, however, the molecules and mechanisms in mDC that are dedicated to NK activation in vivo remain to be understood.

In this study, we focused on the molecules that are induced in mDC during maturation by exposure to double-stranded (ds) RNA and the molecules involved in priming NK cells for target killing (Akazawa et al., 2007a). dsRNA of viral origin and the synthetic analogue polyI:C induce NK activation in concert with mDC in vivo and in vitro (Seya and Matsumoto, 2009). PolyI:C is recognized by the cytoplasmic proteins RIG-I/MDA5 and the membrane protein TLR3, both of which are expressed in mDC (Matsumoto and Seya, 2008). Although RIG-I and MDA5 in the cytoplasm deliver a signal to the adaptor protein IFN promoter stimulator 1 (IPS-1; also known as MAVS, VISA, and Cardif) on the outer membrane of the mitochondria (Kawai et al., 2005; Meylan et al., 2005; Seth et al., 2005; Xu et al., 2005), TLR3 in the endosomal membrane recruits the adaptor protein toll/IL-1 receptor homology domain–containing adaptor molecule 1 (TICAM-1)/TRIF (Oshiumi et al., 2003a; Yamamoto et al., 2003a). Both adaptor proteins activate TBK1 and/or IκB kinase (IKK) ε, which phosphorylate IFN regulatory factor (IRF) 3 and IRF-7 to induce type I IFN (Sasai et al., 2006). We previously showed that the TLR3–TICAM-1 pathway in mDC participates in inducing anti-tumor NK cytotoxicity by polyI:C (Akazawa et al., 2007a). mDC matured with polyI:C can enhance NK cytotoxicity through mDC-NK cell–cell contact (Akazawa et al., 2007a). Therefore, we hypothesized that an unidentified protein is up-regulated on the cell surface of mDC through activation of the TLR3–TICAM-1 pathway, and this protein enables mDC to interact with and activate NK cells. This is the first study identifying an IRF-3–dependent NK-activating molecule, which we abbreviated INAM. INAM is a TICAM-1–inducible molecule on the cell surface of BM-derived DCs (BMDCs) that activates NK cells via cell–cell contact. Our data imply that mDCs harbor a pathway for driving NK activation that acts in conjunction with dsRNA and TLR3.

RESULTS

TICAM-1/IRF-3 signal in BMDCs augments NK activation

An in vitro system for evaluating NK activation through BMDC-NK contact was established for this study (Fig. 1 A). A mouse melanoma cell subline B16D8, which was established in our laboratory as a low H-2 expressor (Mukai et al., 1999), was used as an NK target. PolyI:C, WT BMDC, and NK cells were all found to be essential for NK-mediated B16D8 cytolysis in the in vitro assay (Fig. 1 A). PolyI:C-mediated NK activation was at baseline levels in a transwell with a 0.4-μm pore, suggesting the importance of direct BMDC-NK contact for this cytolysis induction (Fig. 1 A). When WT BMDCs were replaced with TICAM-1$^{-/-}$ BMDCs in this system, polyI:C-mediated NK activation was partly abolished (Fig. 1 B; and Fig. S1, A and B). TICAM-1 of BMDC was involved in driving NK activation, and ultimately B16D8 cells were damaged by BMDC-derived NK cells (Fig. 1 B). PolyI:C-mediated NK activation occurred even when WT NK cells were replaced with TICAM-1$^{-/-}$ NK cells (Fig. 1 B), which means that NK activation barely depends on the TICAM-1 pathway in NK cells.

PolyI:C-activated splenic NK cells were i.p. injected into B6 mice to kill B16D8 cells ex vivo, which is consistent with previous studies (McCartney et al., 2009; Miyake et al., 2009), and this polyI:C-mediated NK activation was markedly reduced in IPS-1$^{-/-}$ mice established in our laboratory (Fig. S1 C), suggesting that NK cell activation is induced via not only the TICAM-1 pathway but also the IPS-1 pathway, which was largely comparable with previous studies (McCartney et al., 2009; Miyake et al., 2009). IPS-1 in BMDC was more involved in polyI:C-driven NK cytotoxicity than TICAM-1 but almost equally contributed to NK-dependent IFN-γ induction to TICAM-1 in our setting (Fig. S1 B). In addition, the serum level of IL-12p40 in polyI:C-treated mice was largely dependent on TICAM-1 (Fig. S1 D; Kato et al., 2006; Akazawa et al., 2007a). In the supernatant of polyI:C-stimulated BMDC and the serum samples from polyI:C-treated mice, IL-12p70 was not detected by ELISA (unpublished data). These results suggest that polyI:C activates NK cells largely secondary to mDC maturation, which is sustained by the IPS-1 or TICAM-1 pathway of mDC. Even though NK cells express TLR3, they are only minimally activated by polyI:C alone. Signaling by TICAM-1 in BMDC can augment NK cytotoxicity and IFN-γ production via BMDC/NK contact.

The TICAM-1 pathway activates the transcription factor IRF-3. More precisely, exogenous addition of polyI:C can activate endosomal TLR3 and cytoplasmic RIG-I/MDA5. RIG-I/MDA5 assembles the adaptor IPS-1, which in turn recruits the NAP1–IKK-ε–TBK1 kinase complex and activates both IRF-3 and IRF-7 (Fitzgerald et al., 2003; Yoneyama et al., 2004). For this reason, we examined the role of IRF-3 and IRF-7 in BMDC for activation of NK cells by polyI:C. Activation of IRF-3, but not IRF-7, was required for BMDC to induce NK cytotoxicity (Fig. 1 C). IL-2 (Zanoni et al., 2005), IFN-α (Gerosa et al., 2002), and trans-presenting IL-15 (Lucas et al., 2007) induced by BMDC are reported to be key cytokines for BMDC-mediated NK activation in response to polyI:C. However, even with normal levels of IFN-α production and IL-15 expression (Fig. 1, D and E), TICAM-1$^{-/-}$ BMDCs failed to induce full NK cytotoxicity (Fig. 1 B). In contrast, IRF-7$^{-/-}$ BMDCs, which have impaired IFN-α and IL-15

Published November 8, 2010

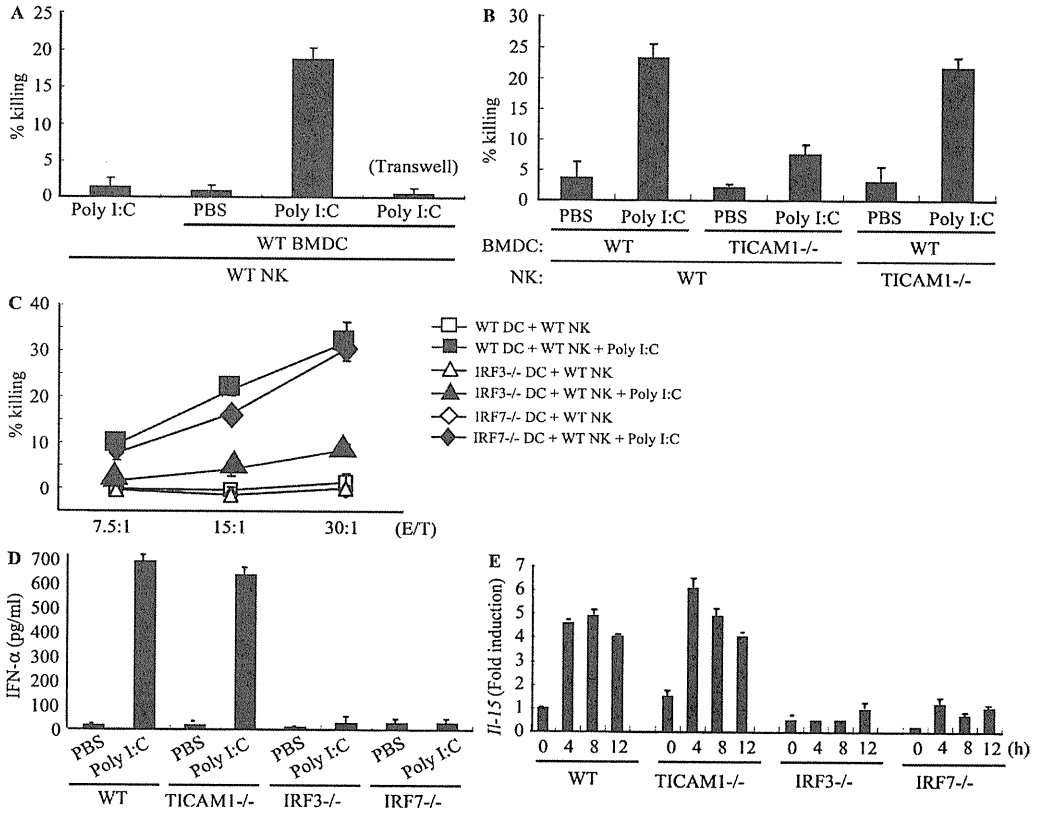

Figure 1. IRF-3 in BMDC controls the capacity to activate NK cells in response to polyI:C. (A and B) WT or TICAM-1$^{-/-}$ NK cells were co-cultured with WT or TICAM-1$^{-/-}$ BMDC in the presence of 10 μg/ml polyI:C for 24 h. NK cytotoxicity against B16D8 was determined by standard ^{51}Cr release assay. E/T = 30. (C) WT NK cells were co-cultured with WT (□, ■), IRF-3$^{-/-}$ (△, ▲), or IRF-7$^{-/-}$ (◇, ◆) BMDC in the presence (■, ▲, ◆) or absence (□, △, ◇) of 10 μg/ml polyI:C for 24 h. NK cytotoxicity against B16D8 was determined by standard ^{51}Cr release assay at the indicated E/T ratio. (D) ELISA of IFN-α in cultures of WT, TICAM-1$^{-/-}$, IRF-3$^{-/-}$, and IRF-7$^{-/-}$ BMDC treated with 10 μg/ml polyI:C for 24 h. (E) Quantitative RT-PCR for IL-15 expression in BMDC stimulated with 10 μg/ml polyI:C. All data are means ± SD of duplicate or triplicate samples from one experiment that is representative of three.

expression, fully activated NK cells (Fig. 1, C–E). Hence, in BDMCs, the TICAM-1–IRF-3 pathway, rather than other cytokines, appears to induce cell surface molecules that mediate BMDC/NK contact and evoke NK cytotoxicity.

Identification of INAM

To identify the NK-activating cell surface molecule on BMDC, we performed microarray analysis on polyI:C-stimulated BMDC prepared from TICAM-1$^{-/-}$ and WT mice. The results yielded nine TICAM-1–inducible molecules with transmembrane motifs (Table S1). Six were induced in an IRF-3–dependent manner, whereas three were still induced in IRF-3$^{-/-}$ BMDC. The NK-activating ability of the products of these genes was investigated by introduction of lentivirus expression vector into IRF-3$^{-/-}$ BMDC. BMDCs with the transduced genes were co-cultured with WT NK cells and polyI:C, and the NK-activating ability was evaluated by determining IFN-γ in the 24-h co-culture. NK cells, but not the gene-transduced BMDCs, produced IFN-γ in the presence of polyI:C. Finally, we identified a tetraspanin-like molecule that satisfied our evaluation criteria (IFN-γ and cytotoxicity) on the mDC-NK activation and named this molecule INAM. INAM clearly differed from other tetraspanins like CD9, CD63, CD81, CD82, and CD151 in the predicted structure. Mouse INAM is a 40–55-kD protein with one N-glycosylation site and possesses four transmembrane motifs (Fig. 2, A and B). Western blotting analysis of INAM-transfected cells under nonreducing conditions showed no evidence of multimers (Fig. 2 B). The N-terminal and C-terminal regions of INAM are in the cytoplasm because anti-Flag antibody did not detect C-terminal Flag-tagged INAM until cells were permeabilized (unpublished data).

Alignment of the predicted amino acid sequence of mouse INAM with that of the human orthologue revealed that the two INAMs shared a 71.7% amino acid identity. INAM is also called FAM26F (Table S1) and is in the FAM26 gene family (Bertram et al., 2008; Dreses-Werringloer et al., 2008). Sequence database searches identified six mouse INAM paralogs. Although FAM26A/CALHM3, FAM26B/CALHM2, and FAM26C/CALHM1 are located on chromosome 19, FAM26D, FAM26E, and FAM26F/INAM are on chromosome 10. Only INAM was inducible with TLR agonists (unpublished data). All FAM26 family proteins have three or four transmembrane motifs predicted by the TMHMM Server (version 2.0). Human CALHM1 has a conserved region (Q/R/N site)

Published November 8, 2010

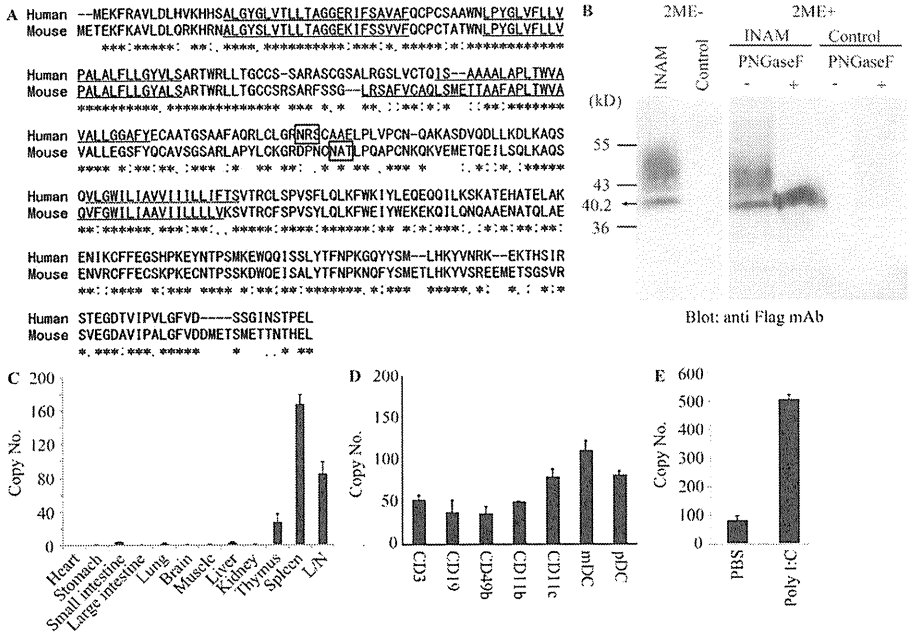

Figure 2. Sequence alignment of INAM and expression of INAM. (A) Sequence alignment of human and mouse INAM. Asterisks, identical residues; double dots, conserved substitutions; single dots, semiconserved substitutions; box, N-glycosylation site; underline, transmembrane motif. (B) Immunoblot analysis of lysates of 293FT cells transfected with plasmid encoding Flag-tagged INAM. PNGase, *N*-glycosidase. 2ME, 2-mercaptoethanol. (C and D) Quantitative RT-PCR for INAM expression in mouse tissue (C) and spleen cells (D). $CD3^+$, $CD19^+$, $DX5^+$, $CD11b^+$, $CD11c^+$, mDC ($CD11c^+PDCA1^+$), and plasmacytoid DC (pDC; $CD11c^+PDCA1^+$) cells were isolated from splenocytes by cell sorting. Data are expressed as copy number per 10^4 copies of HPRT. Data shown are means ± SD of triplicate samples from one experiment that is representative of three. (E) Augmented INAM expression in LN cells after polyI:C stimulation. WT mice were i.p. injected with 100 µg polyI:C or control buffer. After 24 h, inguinal, axillary, and mesenteric LN were harvested and RNA was extracted from the LN cells. The levels of the INAM mRNA were measured by real-time PCR. The results were confirmed in two additional experiments. Data represent mean ± SD.

with ion channel properties at the C-terminal end of the second transmembrane motif that controls cytoplasmic Ca^{2+} levels (Dreses-Werringloer et al., 2008). However, the Q/R/N site was not found in INAM. CALHM1, 2, and 3 are highly expressed in brain. Quantitative RT-PCR revealed that INAM expression was high in spleen and LNs but low in thymus, liver, lung, and small intestine (Fig. 2 C), although expression of the other two FAM26 family members from chromosome 10 was highest in brain (not depicted). All splenocytes examined ($CD3^+$, $CD19^+$, $DX5^+$, $CD11b^+$, $CD11c^+$, mDCs [$CD11c^+PDCA1^-$], and plasmacytoid DCs [$CD11c^-PDCA1^+$]) expressed INAM to some levels (Fig. 2 D). The INAM expression was inducible by polyI:C in LN cells (Fig. 2 E); the induction levels were more prominent in myeloid cells than in lymphocytes in the LNs (Fig. S2 A). $NKp46^+$ and $DX5^+$ NK cells also expressed INAM with low levels and the levels were mildly increased by polyI:C stimulation (Fig. S2 A and not depicted). Notably, only $CD45^+$ cells expressed INAM, which excludes the participation of contaminating stromal cells in the INAM up-regulation (Fig. S2 B).

BMDC INAM activates NK cells

WT and IRF-$7^{-/-}$ BMDCs induced high NK cytotoxicity in response to polyI:C, whereas TICAM-$1^{-/-}$, IPS-$1^{-/-}$, and IRF-$3^{-/-}$ BMDC showed less NK activation (Fig. 1, B and C; and Fig. S1). INAM expression profile by polyI:C stimulation was then examined using WT, IRF-$3^{-/-}$, IRF-$7^{-/-}$, and TICAM-$1^{-/-}$ BMDCs. Stimulation with polyI:C induced INAM at normal levels in IRF-$7^{-/-}$ BMDC but at decreased levels in IRF-$3^{-/-}$ and TICAM-$1^{-/-}$ BMDC (Fig. 3 A). The expression profiles of INAM in polyI:C-stimulated BMDC were in parallel with those inducing NK activation. BMDCs express a variety of TLRs (Iwasaki and Medzhitov, 2004), but other TLR ligands, Pam_3CSK_4 for TLR1/2, Malp2 for TLR2/6, and CpG for TLR9, barely induced INAM on BMDC. High induction of INAM was observed in BMDC stimulated with LPS as well as polyI:C (Fig. 3 B), both of which can activate TICAM-1 to induce IRF-3 and IFN-α activation (Fitzgerald et al., 2003; Oshiumi et al., 2003a,b; Yamamoto et al., 2003a,b). Because INAM is an IFN-inducible gene (Fig. 3 B), INAM induction may be amplified by type I IFNs.

We next examined whether INAM was localized to the cell surface membrane in BMDC. Immunofluorescence analysis showed Flag-tagged INAM on the cell surface of BMDC. Plasma membrane expression of INAM was also confirmed by cell surface biotinylation (Fig. S3). Although the lentivirus inefficiently infected BMDC, GFP expression levels were similar in cells with control virus and those with INAM-expressing virus (Fig. 3 C). Transduction efficiency and expression from the lentivirus vector were adjusted using GFP expression (not depicted), and surface INAM expression was further confirmed with BMDC, NK cells, and INAM-expressing BaF3 (INAM/BaF3) cells, in some cases using polyclonal antibody (Ab) against INAM (Fig. S4).

We then examined whether overexpressing INAM resulted in signaling that directed BMDC maturation and production of cytokines, including IFN-α and IL-12p40, which are reported to enhance NK activity (Gerosa et al., 2002; Sivori et al., 2004; Lucas et al., 2007). The status of INAM-transduced BMDC was assessed by CD86 expression and cytokine production, and no significant differences in these maturation markers were seen in BMDC overexpressing INAM (Fig. S5). In the same setting, no IL-12p70 was

Published November 8, 2010

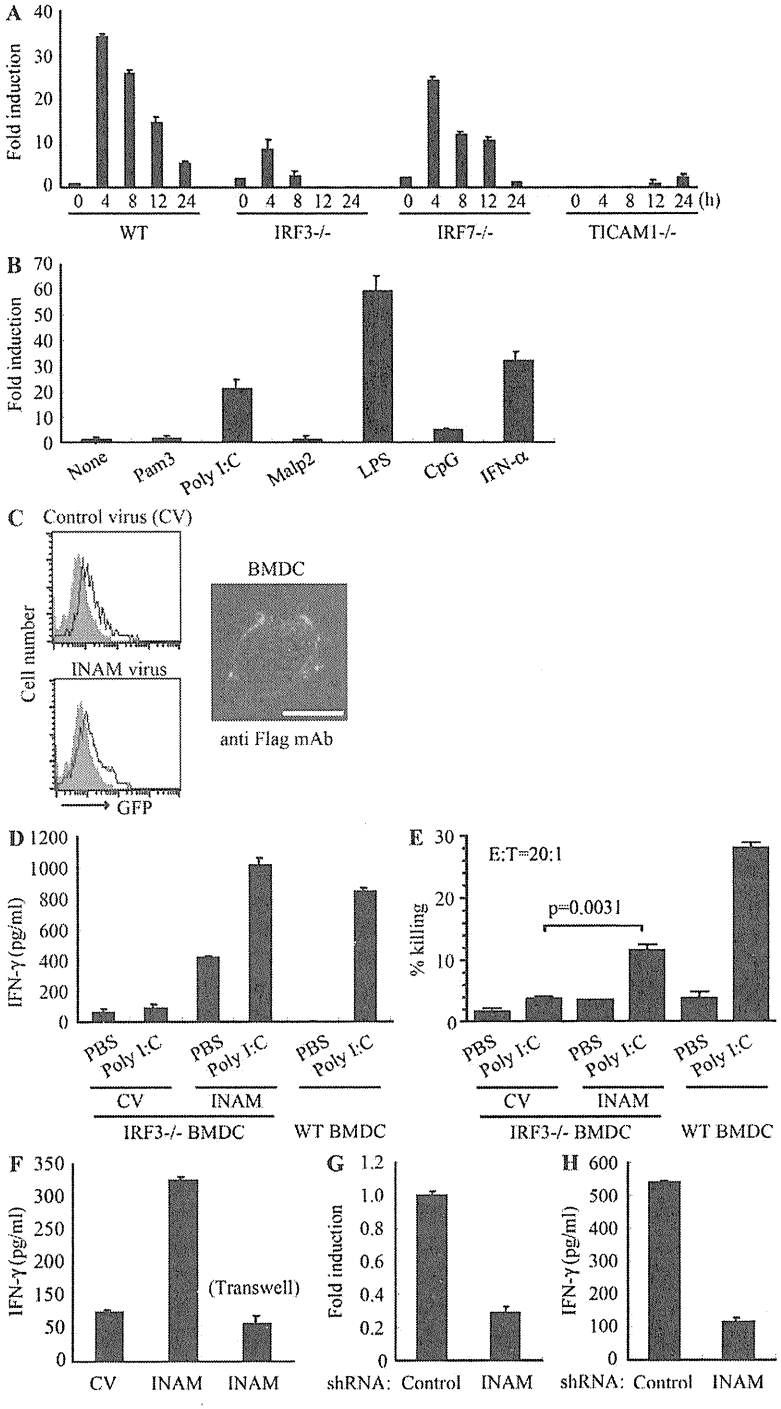

Figure 3. INAM in BMDC participates in DC-mediated NK activation. (A) Quantitative RT-PCR for INAM expression in WT, TICAM-1$^{-/-}$, IRF-3$^{-/-}$, and IRF-7$^{-/-}$ BMDC stimulated with 10 μg/ml polyI:C. (B) Quantitative RT-PCR for INAM expression in WT BMDC stimulated by 100 ng/ml LPS, 10 μg/ml polyI:C, 1 μg/ml Pam3, 100 nM Malp-2, 10 μg/ml CpG, and 2,000 IU/ml IFN-α for 4 h. (C) BMDCs were transduced with Flag-tagged INAM-expressing lentivirus or control lentivirus. GFP expression in the BMDC was determined by flow cytometry, and subcellular localization of INAM was examined by immunofluorescence assay using anti-Flag mAb. Shaded peak, noninfected control; Blank peak, infected BMDC. Bar, 10 μm. (D) ELISA of IFN-γ induced by WT NK cells co-cultured with WT BMDC or IRF-3$^{-/-}$ BMDC transfected with control lentivirus (CV) or INAM-expressing lentivirus (INAM) with/without 10 μg/ml polyI:C. (E) Cytotoxicity against B16D8 by NK cells co-cultured with BMDC transfected with control or INAM-expressing lentivirus with/without 10 μg/ml polyI:C for 24 h. (F) ELISA of IFN-γ induced by WT NK cells co-cultured with IRF-3$^{-/-}$ BMDC transfected with control lentivirus (CV) or INAM-expressing lentivirus (INAM) with 10 μg/ml polyI:C. In some experiments, a transwell was inserted between the INAM-transduced BMDC and NK cells to separate the cells. (G) Quantitative RT-PCR for expression of INAM in BMDC transduced with INAM-shRNA (INAM) or scrambled shRNA (control) and cultured for 48 h. (H) IFN-γ production by WT NK cells determined using ELISA after coculturing with control or the shRNA transfected-BMDC (INAM) and 10 μg/ml polyI:C for 24 h. All data shown are means ± SD of triplicate samples from one experiment that is representative of three.

detected by ELISA (unpublished data). In addition, polyI:C-mediated NK activation occurred in BMDC expressing an INAM mutant lacking the cytoplasmic C-terminal region (193–327 aa; Fig. 4, A and B), excluding the participation of the cytoplasmic region in BMDC maturation signaling.

To investigate whether INAM could reconstitute NK-activating ability in IRF-3$^{-/-}$ BMDC, we transduced INAM into IRF-3$^{-/-}$ BMDC and incubated BMDC with NK cells. Overexpression of INAM in IRF-3$^{-/-}$ BMDC induced NK IFN-γ production and NK cytotoxicity against B16D8, and this NK activation was further enhanced by the addition of polyI:C (Fig. 3, D and E). Thus, polyI:C may also work for NK activation. Direct cell–cell contact with NK cells was required for INAM in IRF-3$^{-/-}$ BMDC to function on enhancing NK activity (Fig. 3 F).

We further confirmed this issue using WT BMDC by shRNA gene silencing. We silenced the INAM gene in BMDC using the lentiviral vector pLenti-dest-IRES-hrGFP and monitored expression by GFP. Because transfection efficiency was relatively high in this case compared with that shown in Fig. 3 C, the expression level of INAM had decreased by ~75% in WT BMDC compared with the nonsilenced control (Fig. 3 G and Fig. S6 A). Although the level of the endogenous INAM protein was not very high, we confirmed that INAM protein was also decreased by shRNA with immunoblotting using anti-INAM pAb (Fig. S7 A). PolyI:C response of BMDC-inducible cytokines tested was not altered by INAM silencing in BMDC (Fig. S6 B). Yet this INAM RNA interference caused a significant decrease in NK cell IFN-γ production after co-culture of the INAM knockdown BMDCs and WT NK cells with polyI:C (Fig. 3 H). Collectively, these results indicate that INAM is downstream of IRF-3 in BMDC and is involved in the activation of NK cells by BMDC.

Published November 8, 2010

Using an INAM-expressing stable BaF3 cell line (INAM/BaF3), we tested the possibility that INAM is an activating ligand for NK cells. As a positive control, we produced a stable BaF3 cell line expressing Rae-1α (Fig. 5 A) which is a ligand for the NK-activating receptor NKG2D (Cerwenka et al., 2000). Although Rae-1α/BaF3 cells were easily damaged by IL-2–activated NK cells, INAM/BaF3 cells were not (Fig. 5 B). In this context, addition of IRF-3$^{-/-}$ BMDC to this culture with BaF3 and NK cells led to slight augmentation of IFN-γ induction irrespective of the presence of INAM on BaF3 cells (Fig. 5 C), and β2-microglobulin$^{-/-}$ BMDC barely affected the IFN-γ level (not depicted). These results suggest that an INAM-containing molecular matrix, rather than INAM alone, acts toward NK cells. Alternatively, INAM may selectively function with specific mDC molecules to activate NK cells.

INAM on NK cells is required for efficient NK activation

mDCs were previously shown to be required for efficient NK activation in vivo and in vitro (Akazawa et al., 2007a). We found that INAM was minimally present in BMDCs and NK cells and that polyI:C acts on both (Figs. S2 A; and Fig 3, D and E). Tetraspanin-like molecules tend to work as scaffolds for heteromolecular complexes that contain molecules functioning in a cis- or trans-adhesion manner to exert intercellular or extracellular functions. Thus, the function of INAM may not be confined to mDC, so we studied the function of INAM on NK cells. In NK cells, INAM was also inducible by polyI:C (Fig. 6 A and Fig. S2 A), and the induction of INAM was abrogated completely in IRF-3$^{-/-}$ NK cells and moderately in TICAM1$^{-/-}$ NK cells (Fig. 6 B). This suggests that polyI:C also acts on NK cells and induces INAM through IPS-1/IRF-3 activation when NK cells are co-cultured with BMDC and polyI:C.

To investigate whether INAM induced in NK cells is associated with BMDC-mediated NK activation, we performed the following experiments (Fig. 6 C). INAM-transduced IRF-3$^{-/-}$ BMDCs were incubated with polyI:C for 4 h, and then the aliquot was mixed with WT NK cells in the presence of polyI:C (Fig. 6 C, left two lanes). A moderate increase of IFN-γ was observed as in Fig. 3 D. In the remainder,

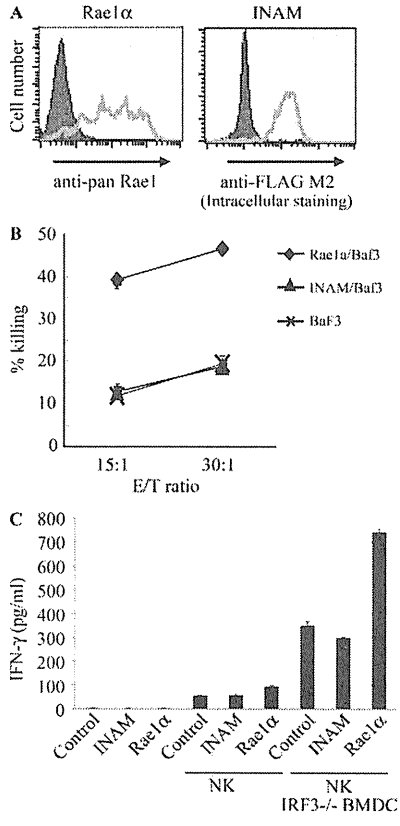

Figure 5. INAM is not an NK-activating ligand. (A) Flow cytometry for Rae-1 and Flag-tagged INAM in stable BaF3 lines. Shaded peak, untransfected control BaF3 staining with anti-pan-Rae-1 Ab or anti-Flag M2 antibody; open peak, stable Rae-1α/BaF3 or stable Flag-tagged INAM/BaF3 staining with anti-pan-Rae-1 antibody or anti-Flag M2 antibody. (B) Cytotoxicity against control BaF3, Rae-1α/BaF3, and INAM/BaF3 by NK cells treated with 1,000 IU/ml IL-2 for 3 d. Data shown are means ± SD of triplicate samples from one experiment representative of three. (C) NK activation is augmented by coexistent BMDC irrespective of INAM expression. NK cells were cultured with 1,000 IU/ml IL-2 for 3 d. 2 × 10^5 NK cells, 10^5 BaF3 cells, and 10^5 IRF-3$^{-/-}$ BMDCs were co-cultured in 200 µl/well and IFN-γ in the supernatants were measured by ELISA. Data show one of two similar experimental results. Data represent mean ± SD.

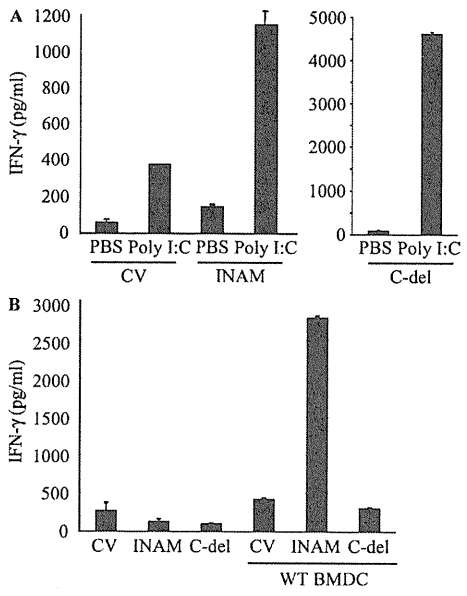

Figure 4. Role of the cytoplasmic tail of INAM. (A) The C-terminal region of INAM was not required for BMDC-mediated NK activation. ELISA of IFN-γ by WT NK cells co-cultured with IRF-3$^{-/-}$ BMDCs transfected with control lentivirus (CV) or a lentivirus expressing intact INAM or a mutant INAM lacking the C-terminus (C-del INAM) with/without 10 µg/ml polyI:C. Data shown are means ± SD of triplicate samples from one experiment representative of three. (B) The cytoplasmic tail of INAM is indispensable for NK IFN-γ induction. INAM or C-del INAM (A) was expressed on IRF-3$^{-/-}$ NK cells. The INAM (or C-del INAM)-expressing IRF-3$^{-/-}$ NK cells were incubated with or without WT BMDC for 24 h. IFN-γ levels in the supernatants were determined by ELISA. One representative result out of several similar experiments is shown. Data represent mean ± SD.